Evolution of Mauna Kea volcano: Inferences from lava compositions recovered in the Hawaii Scientific Drilling Project

H.-J. Yang and F. A. Frey

Department of Earth, Atmospheric and Planetary Sciences, Massachusetts Institute of Technology, Cambridge

J. M. Rhodes

Department of Geology and Geography, University of Massachusetts, Amherst

M. O. Garcia

Department of Geology and Geophysics, University of Hawaii at Manoa, Honolulu

Abstract. The lower 776 m of core recovered during the initial phase of the Hawaii Scientific Drilling Project (HSDP) contains lavas erupted from Mauna Kea volcano. Tholeiitic and alkalic basalts, including an Fe-Ti rich flow, are intercalated in the upper 58 m of Mauna Kea lavas. Similar basaltic sections are subaerially exposed on the lower east flank of Mauna Kea. The Fe-Ti rich lavas reflect large amounts of clinopyroxene, plagioclase, and olivine fractionation within the crust and upper mantle, but the range from tholeiitic to alkalic compositions reflects variable extents of melting of a garnet-bearing source. Based on abundances of incompatible elements, the extent of melting for a basanitoid was a factor of 2 less than that for nearly coeval tholeiitic lavas. All flow units in the lower 718 m of the HSDP core are tholeiitic lavas. Their variability in major element compositions reflect variable accumulation of olivine. Incompatible element abundance ratios in these lavas reflect a complex temporal variation in extent of melting. Within the tholeiitic part of the core, lavas from 800 m to 950 m formed by the largest extent of melting, whereas tholeiitic lavas from the bottom of the core and from just below the tholeiitic to alkalic transition formed by lower degrees of melting. Inferred melt compositions at 16% MgO show that the ~200 to 400 ka Mauna Kea lavas from the HSDP core and the <250 ka subaerial exposures define an inverse correlation between SiO_2 and FeO contents. Based on experimental studies, this correlation is caused by differing pressures of melt segregation. Furthermore, abundances of Nb and SiO_2 are also inversely correlated in these calculated melts. In general, the younger lavas are relatively enriched in FeO and incompatible elements but are depleted in SiO_2. These trends are interpreted to reflect an overall trend of increasing pressure of melt segregation and decreasing extent of melting with decreasing eruption age. There are, however, geochemical variations which indicate short-term reversals in this long-term trend. Previously, the geochemical trends accompanying the transition from tholeiitic to alkalic volcanism at Hawaiian volcanoes have been interpreted as reflecting the effects of increasing distance from the plume axis. The long-term geochemical trends of tholeiitic lavas in the HSDP core also reflect migration of Mauna Kea away from the Hawaiian plume.

Introduction

In order to understand how plume-related volcanism "works," it is imperative to determine how the geochemical characteristics of the lavas vary with time at an individual volcano. This is the major objective of the Hawaii Scientific Drilling Project (HSDP). It is well established that Hawaiian volcanoes evolve through a series of distinct stages with the voluminous shield stage forming more than 95% of each volcano [e.g., *Macdonald et al.*, 1983; *Clague and Dalrymple*, 1987]. As Hawaiian volcanoes evolve from the shield to postshield stage, eruption rates diminish, rift zones become less active, and eruption sites are more widely distributed. This transition is well exposed and consequently

well-studied at large mature Hawaiian volcanoes such as Haleakala [*Chen and Frey*, 1985; *Kurz et al.*, 1987; *West and Leeman*, 1987, 1994; *Chen et al.*, 1990, 1991; *Chen*, 1993), Kohala [*Feigenson et al.*, 1983; *Lanphere and Frey*, 1987; *Hofmann et al.*, 1987; *Spengler and Garcia*, 1988], and Mauna Kea [*West et al.*, 1988; *Frey et al.*, 1990, 1991; *Kennedy et al.*, 1991; *Yang et al.*, 1994; *Wolfe et al.*, 1995]. In these studies the temporal geochemical variations of the lavas have provided constraints on volcanic processes that are important as a Hawaiian volcano moves away from the hotspot.

Temporal geochemical variations during the extended period of shield-stage volcanism are less well known because continuous sections of shield-stage lavas containing a long temporal record are not subaerially exposed on the actively growing shields at Kilauea and Mauna Loa or at the older volcanoes where the shields are largely covered by postshield lavas. It is known, however, that there are important geochemical differences

between shields [e.g., *Tilling et al.,* 1987; *Frey and Rhodes,* 1993] and recent efforts have focused on documenting short- and long-term changes in the geochemistry of shield lavas from Kilauea [e.g., *Hofmann et al.,* 1984; *Tilling et al.,* 1987; *Rhodes et al.,* 1989; *Garcia et al.,* 1992; *Pietruska and Garcia,* 1994; *Chen et al.,* 1996] and Mauna Loa [e.g., *Rhodes,* 1988; *Lipman et al.,* 1990; *Kurz and Kammer,* 1991; *Garcia et al.,* 1995; *Kurz et al.,* 1995; *Rhodes and Hart,* 1995].

A major objective of the HSDP is to determine and interpret temporal geochemical variations of lavas forming the shield of Mauna Kea volcano. Core from the first phase of HSDP recovered 280 m of Mauna Loa flows overlying 776 m of subaerially erupted Mauna Kea lavas ranging in age from ~200 to 400 ka [*Sharp et al.,* this issue]. Geochemical data show that the boundary between Mauna Loa and Mauna Kea flows is abrupt and clearly defined [*Kurz et al.,* this issue; *Lassiter et al.,* this issue; *Rhodes,* this issue]. Our objectives are (1) to compare the Mauna Kea lavas in the drill core with previously studied lavas exposed on the subaerial flanks of the volcano and with a small suite of submarine lavas dredged from the east rift zone at water depths of 1.6 to 3.3 km; and (2) to identify and interpret the compositional variations of Mauna Kea lavas in this drill core.

Previous Studies of Mauna Kea Volcano

At 4205 m above sea level, Mauna Kea is the tallest of the five shield volcanoes composing the island of Hawaii. The subaerially exposed portion of the volcano has been the focus of several petrologic and geochemical studies [*West et al.,* 1988; *Frey et al.,* 1990, 1991; *Fodor and Vandermeyden,* 1988; *Kennedy et al.,* 1991; *Wolfe et al.,* 1995]. Postshield lavas erupted from widely scattered vents cover most of the subaerial surface of the volcano. The subaerially exposed Mauna Kea lavas have been divided into two stratigraphic units: a lower basaltic sequence, Hamakua Volcanics; and an upper hawaiite to mugearite sequence, Laupahoehoe Volcanics [*Langenheim and Clague,* 1987]. Although a large and precise database for ages is not available, Hamakua lavas range in age from approximately 250 to 70 ka, and Laupahoehoe lavas range from approximately 65 to 4 ka [*Wolfe et al.,* 1995].

The Laupahoehoe lavas are evolved alkalic lavas, hawaiites, and mugearites with <4.5% MgO [*West et al.,* 1988; *Wolfe et al.,* 1995]. These lavas are nearly aphyric with only rare olivine and plagioclase phenocrysts/xenocrysts, but some lavas contain xenoliths of dunite and gabbro [*Fodor and Vandermeyden,* 1988]. There is a distinct compositional gap between the Laupahoehoe hawaiites and Hamakua basalts [*Frey et al.,* 1990]. The Laupahoehoe Volcanics, which contain no basaltic lavas, formed when magma supply rates were insufficient to maintain conduits for ascent of basaltic magma. That is, as Mauna Kea moved away from the long-term source of basaltic magma, the mantle plume, basaltic magma ponded at depth, perhaps at the mantle-oceanic crust boundary. As this basaltic magma cooled, it formed a dense clinopyroxene-rich mineral assemblage containing Fe-Ti oxides similar to some of the gabbroic xenoliths in Laupahoehoe lavas [*Fodor and Vandermeyden,* 1988; *Kennedy et al.,* 1991]. Segregation of this mineral assemblage created residual hawaiitic magmas which were sufficiently buoyant to erupt [see *Frey et al.,* 1990, Figure 15].

Studies of Hamakua lavas have focused on stratigraphic sections from (1) the well-exposed and arid northwest flank, ~75 flows ranging in age from ~81 to 150 ka [*Frey et al.,* 1990]; (2)

the south flank at elevations of 2750 to 3100 m, where Hamakua lavas directly underly Laupahoehoe lavas in Waikahalulu Gulch [see *Frey et al.,* 1990, Figure 2]; and (3) the windward, east flank where the oldest subaerially exposed Hamakua lavas outcrop in deep, 90 to 165 m, gulches formed by stream erosion [*Frey et al.,* 1991].

The Waikahalulu Gulch high on the south flank is an important section because it includes Laupahoehoe lavas, 31±9 ka, which directly overlie 12 evolved (5-6% MgO) alkalic Hamakua basalts. The lower five Hamakua lavas in this gulch are, however, tholeiitic basalts with 7-10% MgO. One of these lavas has a K/Ar age of 153±38 ka [*Wolfe et al.,* 1995]. The near sea level sections on the east flank are dominantly intercalated alkalic and tholeiitic basalts, with some flows of ankaramite, picrite, and evolved Fe-Ti-rich alkalic lavas. An alkalic basalt (sample La-7) in one of these sections has a K/Ar age of 237±31 ka [*Wolfe et al.,* 1995]. The intercalated tholeiitic and alkalic basalts in these sections have similar radiogenic isotopic ratios of Sr, Nd, and Pb [*Kennedy et al.,* 1991]. *Frey et al.* [1991] concluded that these tholeiitic and alkalic basalts were formed from a garnet-bearing peridotite by different extents of melting. They also concluded that none of the MgO-rich picrites and ankaramites are representative of high MgO melts. Based on mineral and whole rock compositions and petrography, these lavas are best explained as complex mixtures of relatively evolved melts and accumulated olivine and clinopyroxene phenocrysts and xenocrysts. The evolved Fe-Ti-rich Hamakua lavas formed as residual melts after segregation of an olivine, clinopyroxene, and plagioclase-bearing assemblage [*Frey et al.,* 1991], but they followed a very different liquid line of descent than Laupahoehoe lavas; most notably, Fe-Ti oxide was not an important fractionating phase during formation of the Hamakua Volcanics.

Submarine tholeiitic lavas dredged from the east rift of Mauna Kea have also been studied [*Garcia et al.,* 1989; *Frey et al.,* 1991; *Yang et al.,* 1994]. Because they erupted far from the volcano summit, these submarine lavas are presumed to be the oldest lavas recovered from the Mauna Kea shield. Based on their vesicularity, depth below sea level, and subsidence rates, *Wolfe et al.* [1995] estimated an eruption age of 400 ka for these submarine lavas. These lavas are MgO-rich, 11-20%, but like subaerially erupted picrites, they are not representative of crystallized MgO-rich melts. Their whole rock and mineral compositions reflect mixing of an evolved magma, <7% MgO, with a magma containing abundant olivine xenocrysts. The submarine sample, SU 22-64, dredged from the greatest depth and most distant from the summit is transitional in composition; that is, it has relatively lower SiO_2 content and higher abundances of incompatible elements, and it may have formed by a relatively lower extent of melting [*Yang et al.,* 1994].

Results

Major Elements

Abundances of major elements were determined by X ray fluorescence (XRF) [*Rhodes,* this issue], and trace element abundances were determined by neutron activation and XRF (Table 1 and *Rhodes* [this issue]). Sample numbers in Table 1 indicate the core run and depth in meters within this core run [see *Hawaii Scientific Drilling Project,* 1994]. In general, only one sample from each core run was analyzed, and we identify samples by their core run number. The whole rock major and trace

Table 1. Trace Element Abundances in HSDP Lavas

	Mauna Loa Samples					Mauna Kea Samples										
	055-0.75	117-0.80	133-6.10	142-1.60	153-3.05	158-0.05	159-4.10	160-5.75	164-1.55	166-5.25	167-1.30	169-3.55	171-4.55	174-0.55	174-9.65	177-2.60
Depth, m	74.0	184.4	223.1	241.1	268.2	281.3	285.5	289.0	299.2	305.7	307.7	314.5	320.6	324.6	327.4	331.7
Flow unit	11	27	34	37	43	45	47	47	49	51	52	54	55	57	57	58
Sc	26.2	29.2	24.5	27.8	25.8	30.1	32.9	29.7±.2	29.6	29.5	29.1	31.4	30.8	30.8	30.9	25.5
Cr	670	260	864	620	856	783	635	911±3	127	141	143	175	1039	98	99	127
La	7.56	6.90	5.94	7.10	6.84	17.7	19.7	17.5±.1	19.0	21.4	21.2	16.3	10.8	27.3	28.0	23.7
Ce	20.2	19.6	16.3	18.7	17.7	42.4	45.9	41.1	46.4	49.6	50.9	41.0	26.5	67.4	67.6	59.3
Nd	13.1	13.1	11.0	13.2	13.0	26.1	28.3	25.9±.6	28.7	30.5	30.9	26.8	18.8	41.3	42.5	36.5
Sm	3.86	3.97	3.29	3.98	3.63	6.82	7.63	6.75±.08	7.15	7.77	7.47	6.94	4.96	10.4	10.35	9.00
Eu	1.44	1.50	1.23	1.46	1.39	2.32	2.60	2.31±.01	2.59	2.67	2.62	2.40	1.70	3.47	3.48	3.13
Tb	0.61	0.75	0.53	0.65	0.61	1.00	1.19	1.03±.08	1.02	1.14	1.11	1.07	0.83	1.61	1.56	1.31
Yb	1.62	1.90	1.47	1.75	1.52	2.10	2.19	1.98±.05	2.13	2.29	2.30	2.15	1.58	3.07	3.00	2.40
Lu	0.22	0.29	0.21	0.27	0.25	0.28	0.31	0.28±.01	0.31	0.32	0.33	0.31	0.25	0.40	0.42	0.33
Hf	2.68	2.78	2.27	2.81	2.65	4.83	5.45	4.85±.04	5.25	5.54	5.51	4.95	3.48	7.64	7.46	6.58
Th	0.27	0.46	0.16	0.47	-	0.91	1.33	1.24±.20	0.91	1.40	1.14	0.91	0.63	1.97	1.79	1.51

	Mauna Kea Samples															
	180-5.90	185-3.95	189-8.50	193-3.90	202-1.40	208-5.20	212-0.40	224-1.75	229-0.05	250-0.00	251-3.90	259-0.75	287-3.15	291-0.05	303-3.00	311-0.70
Depth, m	342.0	354.5	367.6	378.3	400.3	415.7	424.1	459.4	472.7	526.6	530.9	542.2	594.1	603.8	623.3	645.0
Flow unit	59	62	64	69	72	75	76	89	91	106	107	109	119	120	126	131
Sc	29.7	30.7	19.9±.3	22.7±.1	29.9	29.3±.1	22.6	29.6	27.4	26.7	29.4	23.0	31.3	30.3	22.5	29.6
Cr	440	313	1865±9	1380±20	209	552±3	1304	423	875	920	364	1540	333	688	1393	586
La	14.3	14.8	5.72±.13	8.45±.02	12.8	15.1±.1	7.76	12.9	10.7	11.0	13.6	7.55	13.4	10.3	8.22	9.55
Ce	36.6	36.9	14.8±.4	22.2±.8	33.8	37.9±.4	20.1	32.7	27.1	27.8	34.2	19.5	34.8	25.9	20.3	24.4
Nd	24.4	24.2	9.80±.42	14.5±.5	22.2	24.6±.2	13.7	21.1	18.0	17.9	21.4	13.0	23.3	17.5	14.9	17.2
Sm	6.50	6.45	2.69±.01	4.07±.09	6.03	6.35±.01	3.71	6.18	4.87	4.94	5.48	3.75	6.24	4.95	3.87	4.62
Eu	2.25	2.27	0.98±.01	1.46±.01	2.12	2.20±.03	1.32	2.20	1.78	1.74	2.00	1.36	2.22	1.78	1.40	1.69
Tb	1.05	1.13	0.41±.08	0.64±.01	1.00	1.00±.04	0.59	1.04	0.80	0.79	0.87	0.64	0.98	0.83	0.66	0.85
Yb	2.10	2.15	0.96±.02	1.37±.04	2.17	1.76±.10	1.38	1.99	1.69	1.59	1.94	1.29	2.14	1.72	1.31	1.93
Lu	0.29	0.30	0.14±.01	0.20±.01	0.29	0.27±.01	0.19	0.30	0.25	0.23	0.26	0.18	0.29	0.24	0.18	0.27
Hf	4.49	4.64	1.87±.02	2.88±.10	4.23	4.31±.18	2.69	4.37	3.70	3.69	3.91	2.57	4.80	3.58	2.75	3.37
Th	0.84	0.91	0.43	0.47±.04	0.79	0.88±.23	0.48	0.85	0.63	0.63	0.93	0.79	1.09	0.68	0.62	0.56

Table 1. (continued)

Mauna Kea Samples

	315-3.35	319-1.30	322-3.50	327-2.80	340-5.15	347-6.35	350-2.45	356-1.45	365-0.05	371-0.30	374-5.90	379-3.80	382-4.35	385-5.55	399-4.30	401-4.90
Depth, m	658.2	669.4	677.6	689.8	720.3	738.7	747.4	759.7	781.2	797.4	798.6	821.4	829.2	835.6	869.1	875.4
Flow unit	132	137	138	141	147	152	153	155	159	164	165	167	169	170	176	177
Sc	25.1	24.7±.4	24.6	31.1	25.8	20.9±.3	30.7	30.3	21.8	23.7	22.0±.5	30.3	22.4	31.3	30.4	29.3
Cr	906	989±12	1030	338	867	1420±40	326	413	1450	1020	1460±40	565	1334	412	536	638
La	11.6	9.42±.09	8.27	12.4	11.1	7.23±.12	12.3	11.8	7.56	9.33	7.29±.11	9.03	7.85	10.0	11.9	9.52
Ce	29.6	24.2±1.1	20.9	31.1	28.4	18.2±.7	31.5	30.9	19.3	22.9	19.7±.4	23.5	19.9	26.0	30.2	24.4
Nd	19.3	16.2±0.2	14.2	21.3	18.9	12.0±.5	21.2	21.0	13.8	15.6	12.4±.2	16.6	13.0	17.3	21.3	17.9
Sm	5.30	4.43±.07	3.89	5.70	4.75	3.32±.06	5.71	5.62	3.58	4.13	3.46±.06	4.65	3.82	5.10	5.70	4.60
Eu	1.86	1.57±.02	1.44	2.04	1.71	1.20±.01	2.03	2.00	1.28	1.48	1.26±.02	1.66	1.38	1.84	2.00	1.71
Tb	0.82	0.71±.02	0.63	0.90	0.91	0.55±.01	0.99	0.93	0.64	0.73	0.55±.05	0.81	0.65	0.89	0.88	0.87
Yb	1.69	1.52±.05	1.60	1.92	1.67	1.15±.03	1.88	1.94	1.32	1.48	1.20±.02	1.83	1.35	1.90	2.12	1.77
Lu	0.26	0.22±.01	0.22	0.29	0.26	0.17±.01	0.27	0.27	0.16	0.21	0.17±.01	0.29	0.21	0.26	0.30	0.26
Hf	3.67	3.16±.05	2.83	4.21	3.39	2.41±.02	4.09	4.01	2.51	2.95	2.50±.02	3.34	2.77	3.55	3.88	3.38
Th	0.77	0.66±.04	0.62	0.91	0.62	0.51±.09	0.71	0.94	0.30	0.38	0.54±.07	0.61	0.64	0.56	0.66	0.66

Mauna Kea Samples

	424-9.30	428-2.70	434-7.90	442-2.10	446-2.40	452-3.90	457-4.30	463-6.00	464-7.10	466-5.00	Precision, %	KIL 1919
Depth, m	939.2	946.3	965.2	983.9	994.7	1009.5	1024.6	1043.7	1047.1	1052.4		
Flow unit	196	197	203	208	211	218	220	224	225	227		
Sc	29.1±.3	30.7	25.3	21.3	25.3	29.7	27.5	26.8±.1	27.2	26.9	1	30.9
Cr	479±3	393	838	1456	1005	364	690	720±2	752	664	1	249
La	9.33±.09	11.2	8.74	7.21	11.2	12.1	12.7	12.0±.04	11.8	12.8	1	15.2
Ce	24.5±.6	28.6	22.2	18.3	29.1	31.6	31.6	30.8±.9	30.6	32.8	3	38.0
Nd	16.7±.8	20.5	15.4	12.7	18.6	20.4	20.8	19.8±.2	19.3	21.5	3	23.8
Sm	4.54±.03	5.43	4.24	3.53	5.01	5.69	5.46	5.26±.04	5.25	5.60	1	5.90
Eu	1.67±.01	1.95	1.55	1.24	1.73	2.01	1.96	1.91±.02	1.87	1.98	1	2.06
Tb	0.82±.03	0.95	0.73	0.60	0.87	0.99	0.90	0.88±.01	0.91	0.78	6	0.88
Yb	1.75±.01	2.01	1.74	1.33	1.85	2.00	1.86	1.74±.01	1.79	1.86	2	1.94
Lu	0.26±.01	0.28	0.24	0.18	0.26	0.26	0.25	0.25±.01	0.25	0.26	3	0.27
Hf	3.42±.11	3.83	3.08	2.50	3.63	3.95	4.02	3.85±.01	3.82	4.05	2	4.32
Th	0.63±.01	0.70	0.44	0.68	1.01	0.84	0.78	0.85±.08	0.75	0.84	12	1.14

Trace element abundances are given in parts per million. These samples are aliquots of the powders analyzed for major and other trace elements by *Rhodes* [this issue]. Sample number indicates core run and depth in meters within each core. These abundances were determined by instrumental neutron activation at the Massachusetts Institute of Technology. Co and Ta data are not reported because samples were ground in WC. Data for the Mauna Loa lavas are discussed by *Rhodes* [this volume]. Precision (one sigma) of the data is indicated by replicate analyses of nine HSDP samples, and the average one-sigma precision is indicated in the column labeled "precision." Accuracy can be assessed from the data for KIL 1919. This sample is from the same flow as USGS standard Hawaiian basalt BHVO-1, and it was prepared by H. West and distributed as a standard rock for those analyzing the HSDP core. Except for Cr this sample has trace element abundances very similar to that of BHVO-1. The data are a mean of 21 NA analyses made during 1994. Based on a comparison of these data with nine analyses of BHVO-1 by isotope dilution made at the Max Planck Institut für Chemie, we have lowered our Ce abundances by 5.3%. To be consistent with this HSDP data, our previous NA data for Ce in Hawaiian lavas should be lowered by 5.3%.
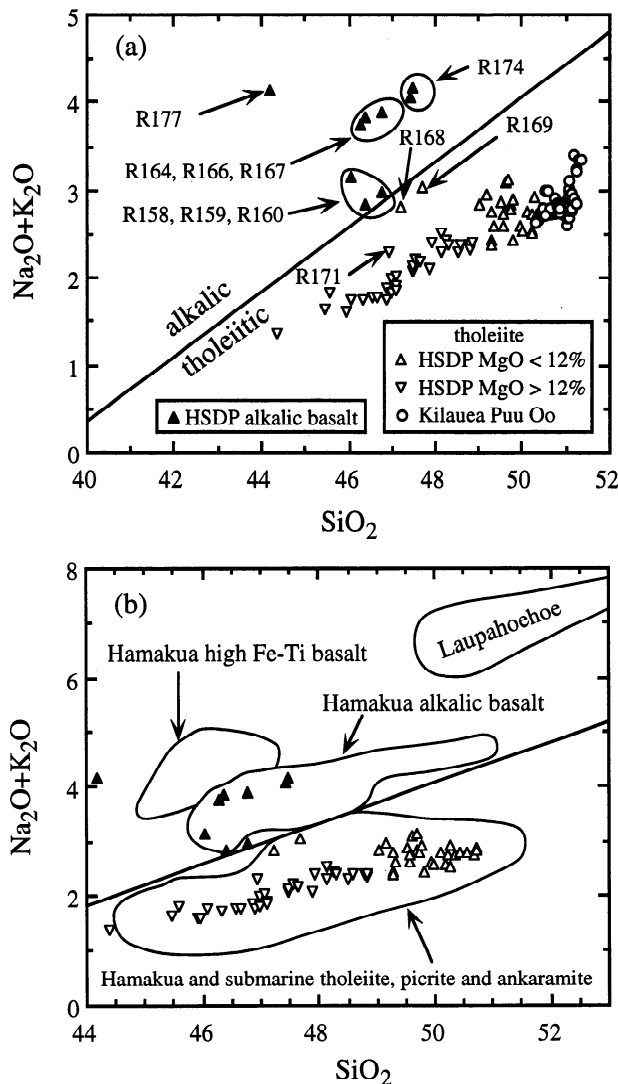
Figure 1. Abundances of $Na_2O + K_2O$ versus SiO_2 content (all in weight percent) with FeO as 0.85 of total iron. Alkalic-tholeiitic dividing line from *Macdonald and Katsura* [1964] and is given by $Na_2O + K_2O = 0.37$ SiO_2-14.43. HSDP lavas with K_2O/P_2O_5 <1.6 have lost K_2O during posteruptive alteration (see text); therefore the K_2O contents of these lavas were increased so that $K_2O/P_2O_5 = 1.6$, the average value for unaltered HSDP lavas. (a) HSDP lavas - alkalic lavas from the upper 58 m of core are labeled. At high SiO_2, HSDP tholeiitic lavas overlap with recent Kilauea lavas [*Garcia et al.*, 1992]. In Figure 1a and all subsequent figures, alkalic and tholeiitic HSDP lavas are indicated by solid and open triangles, respectively. (b) HSDP lavas compared to fields for subaerially exposed Mauna Kea lavas and lavas dredged from the submarine east rift. None of the HSDP lavas are similar to the Laupahoehoe Volcanics. Most HSDP lavas (R177 is an exception) overlap with the fields for Hamakua Volcanics. In this and subsequent figures, HSDP data are from this paper and *Rhodes* [this issue], submarine lava data from *Yang et al.* [1994] Hamakua and Laupahoehoe data from *West et al.* [1988] and *Frey et al.* [1990, 1991].

element data obtained for Mauna Loa lavas in the upper 280 m of the HSDP core are discussed by *Rhodes* [this issue]. In this paper we discuss the compositions of Mauna Kea lavas ranging from R158 at 281.3 m to R466 at 1052.4 m in the HSDP core. These

lavas range from basaltic to picritic; no highly evolved lavas with <5.4% MgO are present. A total alkalies (Na_2O+K_2O) versus SiO_2 content plot shows the gradual transition from tholeiitic to alkalic basalt as shield building ends (Figure 1). Note that we use this plot to define alkalic and tholeiitic basalts, but *Wolfe et al.* [1995] defined tholeiitic basalt as having normative quartz, transitional basalt as having normative olivine and hypersthene and alkalic basalt as having normative nepheline. In Figure 1b, lavas from the HSDP core, except for R177 from flow unit 58, overlap with the fields defined by the Hamakua Volcanics and submarine lavas from the east rift, but none of the HSDP lavas are similar to the Laupahoehoe Volcanics.

Lavas from deeper than 342 m in the HSDP core, samples R180 to R466 (from flow units 59 to 227), lie well within the tholeiitic field forming an elongated field that overlaps with recent Kilauea lavas at 50 to 51% SiO_2 (Figure 1a). Many of these tholeiitic Mauna Kea lavas are MgO-rich (12 to 28.2%), and they contain abundant olivine [*Baker et al.*, this issue; *Garcia*, this issue]. The trend of these high-MgO lavas to low SiO_2 contents is subparallel to the tholeiitic-alkalic dividing line (Figure 1), and it is consistent with accumulation of olivine. The uppermost Mauna Kea lavas in the HSDP core, ranging from R158 in flow unit 45 at 281.3 m to R177 in flow unit 58 at 331.7 m, are compositionally diverse; 11 of the 12 samples from this part of the core plot close to or in the alkalic field (Figure 1a). However, only one sample, R177, has more than 1% normative nepheline. The youngest Mauna Kea samples (R158, R159, and R160 from flow units 45 and 47 and spanning a range of 7.7 m) form a group of alkalic lavas close to the alkalic-tholeiitic boundary. The underlying three samples (R164, R166, and R167 in flow units 49, 51, and 52 from the next 18.7 m of core) have significantly higher $Na_2O + K_2O$, and they plot well within in the alkalic field. Below these alkalic lavas three samples (R168, R169, and R171 in flow units 53, 54, and 55 from 7.7 m of core) plot in the tholeiitic field, but in relation to the main trend they are offset to higher alkali contents (Figure 1a). Below these marginally tholeiitic lavas are two thick units of aphyric alkalic lavas. The R174 samples from flow unit 57 have the lowest MgO contents, ~5.5%, found in the core, whereas sample R177 from flow unit 58 is a basanitoid with 8.2% MgO. The latter sample is in the basanite field on a total alkalis versus SiO_2 plot [*Le Bas et al.*, 1992], and it has 5.5% normative nepheline with FeO = 0.85 total iron, but it does not have modal nepheline. In summary, the transition from tholeiitic to alkalic volcanism in the HSDP core was gradual over a time span of at least 42 ka [*Sharp et al.*, this issue] and includes ~50 m of core where basalts of varying alkalinity are intercalated (Figure 2a).

Important aspects of the compositional variations among the Mauna Kea HSDP lavas are apparent in MgO variation plots (Figure 3). Lavas from the lower parts of the core (429-1052 m) define an inverse SiO_2-MgO trend (Figure 3a). In contrast, at a given MgO content the nine alkalic lavas in the upper part of core are offset to lower SiO_2 and higher Fe_2O_3 (total iron); sample R177 has the lowest SiO_2 and highest Fe_2O_3 content (Figures 3a and 3b). The three marginally tholeiitic lavas (R168, R169, and R171) intercalated with the alkalic lavas are also offset to lower SiO_2 contents (Figure 3a). In addition, within the 100-m interval below the alkalic lavas, there are three high-MgO tholeiitic lavas (R189, R193, and R212) which are offset from the main trend of the tholeiitic lavas to lower SiO_2 and higher Fe_2O_3 (Figures 3a and 3b).

Abundances of Al_2O_3 are inversely correlated with MgO, and the slope is also consistent with accumulation of olivine (Fo_{86})
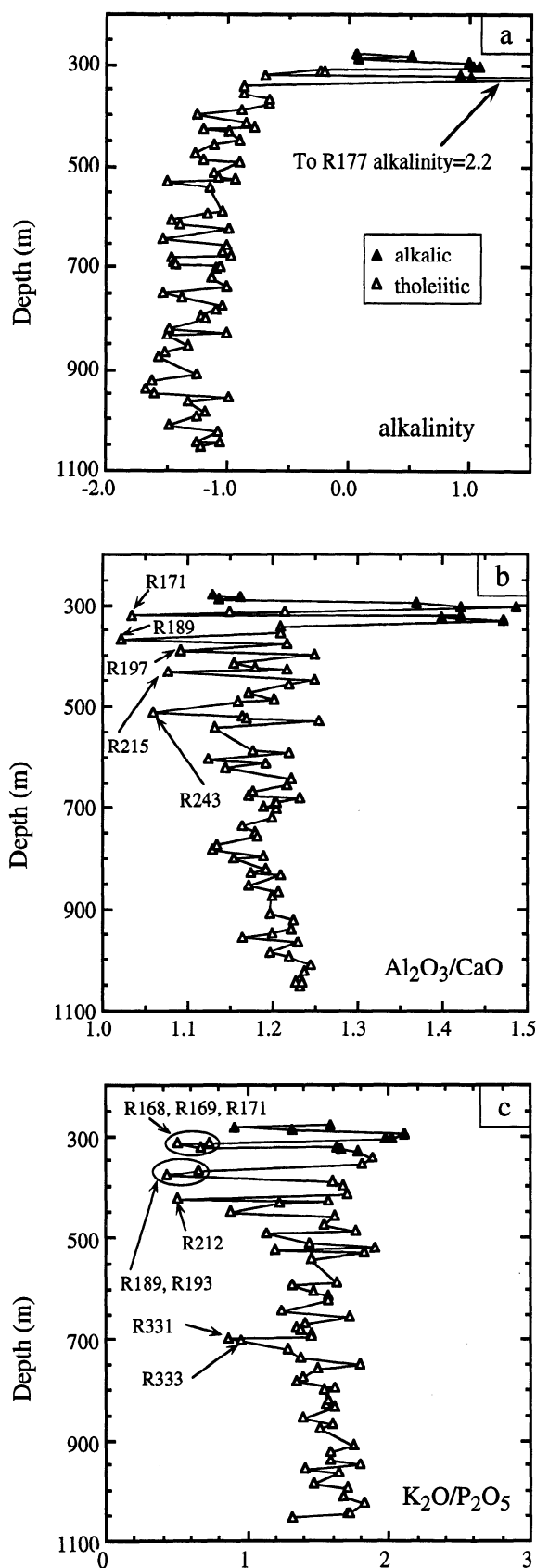
Figure 2. (a) Alkalinity, (b) Al_2O_3/CaO and (c) K_2O/P_2O_5 in Mauna Kea lavas versus depth in the HSDP core. Alkalinity is the vertical distance from the tholeiitic-alkalic dividing line in Figure 1. Lavas with atypically low Al_2O_3/CaO and K_2O/P_2O_5 are labeled.

(Figure 3c and *Baker et al.* [this issue]). The negative Al_2O_3-MgO trend is characteristic of Hawaiian lavas and opposite to the trends defined by mid-ocean ridge basalts which are controlled in part by plagioclase fractionation [e.g., *Langmuir et al.*, 1992]. In detail, however, several of the alkalic basalts are offset to slightly higher Al_2O_3. The HSDP lavas with more than 7% MgO also show an inverse relationship between CaO and MgO abundances (Figure 3d). The five most evolved HSDP lavas are alkalic (R174-0.55, R174-9.65, R167, R166, and R164 with 5.4 to 6.3% MgO); in relation to the CaO-MgO trend of the higher MgO lavas, these alkalic lavas have lower CaO and correspondingly high Al_2O_3/CaO of ~1.4. The Al_2O_3/CaO ratio ranges from 1.13 to 1.25 in all lavas from the lower 539 m of core and in 62 of the 73 Mauna Kea lavas analyzed (Figure 2b). This range is similar to that of historical tholeiitic lavas with >7% MgO from Kilauea (1.08 to 1.27), but lower than historical tholeiitic lavas from Mauna Loa (1.27 to 1.34) [*Frey and Rhodes*, 1993]. The considerable variation of Al_2O_3/CaO in the upper 232 m of Mauna Kea lavas reflects the five evolved lavas with Al_2O_3/CaO ~1.4, basanitoid R177 with Al_2O_3/CaO = 1.47, and five MgO-rich lavas, R171, R189, R197, R215, and R243 which have atypically low ratios of 1.02 to 1.10 (Figure 2b).

Abundances of TiO_2, Na_2O, and P_2O_5 are also inversely correlated with MgO (Figures 3e, 3f, and 3g), but nine alkalic samples from the upper 50 m of Mauna Kea lavas are offset to higher abundances, with maximum TiO_2 content of 4.5% in sample R174 and Na_2O content of 3.24% in sample R177. These samples also have the highest P_2O_5 contents (Figure 3g).

Incompatible Trace Elements

Abundances of highly and moderately incompatible elements, such as Th, Ba, Nb, La, Sm, and Zr, are highly correlated in all Mauna Kea lavas (Figure 4). These trends show that during the petrogenesis of Mauna Kea lavas the order of increasing incompatibility was heavy rare earth element (HREE)-Sm-Zr-light REE (LREE)-Nb-Ba-Th. Within the HSDP core the nine alkalic lavas in the upper 58 m of the Mauna Kea section have the highest abundances of incompatible elements; these abundances overlap the range of previously studied Hamakua alkalic lavas (Figure 4).

Chondrite-normalized abundances of rare earth elements (REE) are typical of Hawaiian tholeiitic and alkalic lavas (Figure 5). Light REE contents are quite variable, $(La)_N = 25$ to 117 with $(La/Ce)_N \geq 1$ in alkalic lavas and ~1 in tholeiitic lavas (N is chondrite-normalized). Abundances of heavy REE, such as Yb, are also variable $(Yb)_N = 5.5$ to 18.1, but this variability is largely a result of olivine accumulation. Normalization of the 31 tholeiitic HSDP lavas with 7.4 to 16% MgO to MgO = 16% by olivine addition yields a mean Yb content of 1.6 ± 0.1 ppm [also see *Feigenson et al.*, this issue; *Hofmann and Jochum*, this issue].

In the HSDP lavas, abundance ratios involving elements of similar incompatibility do not vary systematically with abundances of incompatible elements; e.g., Zr/Hf varies only from 38.7 to 44.4 and La/Nb from 0.80 to 0.91 with sample R371 = 0.765 (Figures 6a and 6c). The high-precision Th data for HSDP lavas obtained by isotope dilution [*Lassiter et al.*, this issue] yield a quite uniform Nb/Th ratio of 17.4 ± 1.4 (Figure 6b), overlapping with the ratio 15.5 ± 1.7 previously reported for 20 Hamakua lavas [*Kennedy et al.*, 1991]. Like other Hawaiian shields, Mauna Kea lavas have a uniform Nb/Th ratio which differs from the bulk earth estimate of 8.6; this difference has been used to argue against a primitive mantle component in
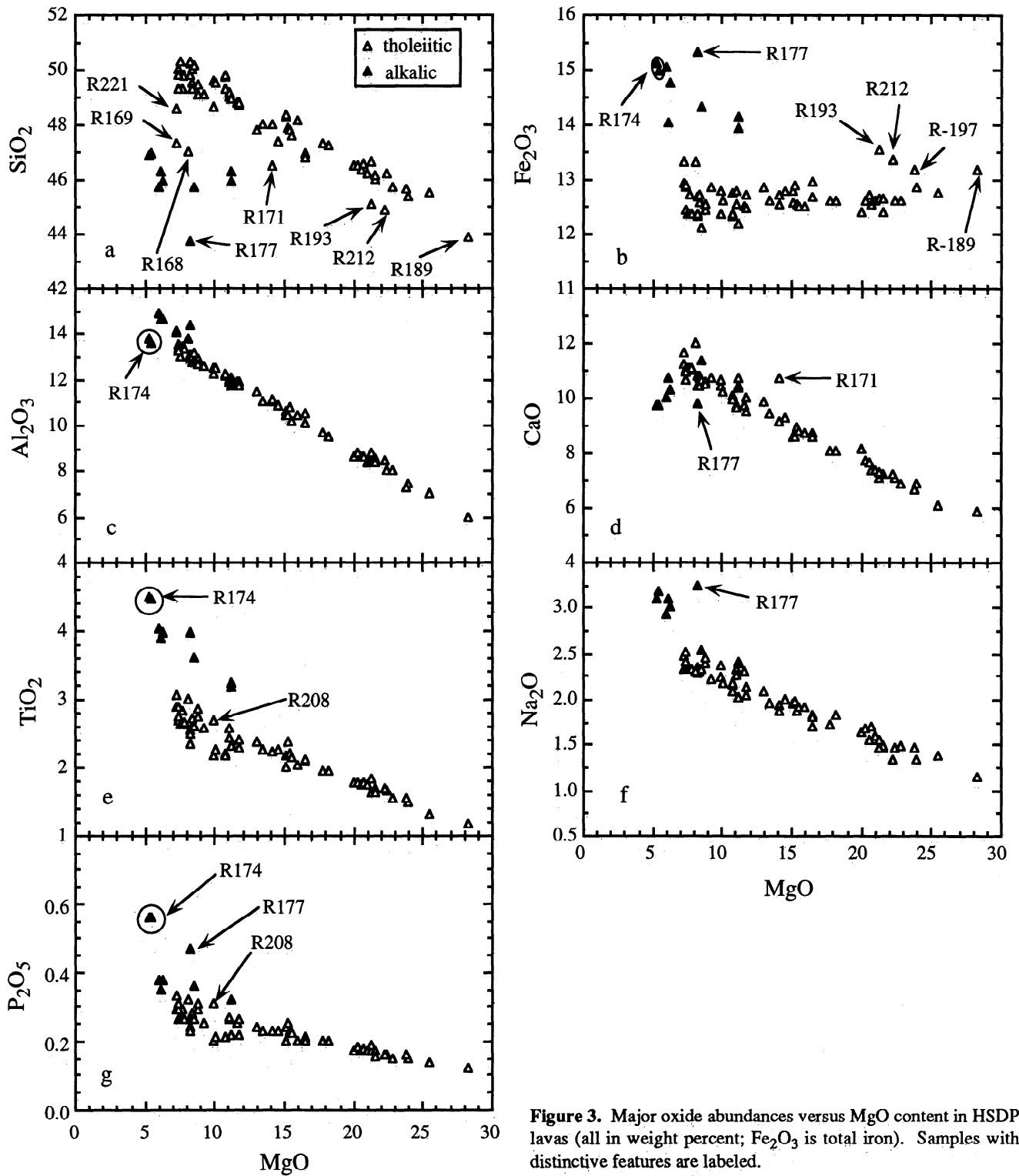
Figure 3. Major oxide abundances versus MgO content in HSDP lavas (all in weight percent; Fe_2O_3 is total iron). Samples with distinctive features are labeled.

Hawaiian shield lavas [*Hofmann*, 1986; *Frey et al.*, 1994; *Hofmann and Jochum*, this issue].

In contrast, abundance ratios involving elements of different incompatibility, such as La/Sm, La/Yb, and Zr/Nb, vary systematically with abundances of a highly incompatible element, such as Nb (Figure 6). The nine alkalic lavas within the upper 50 m of the Mauna Kea section (281 to 332 m) have the highest La/Yb and lowest Zr/Nb (Figure 7); these ratios overlap with those of the previously studied alkalic Hamakua lavas (Figure 8).

Although this part of the core is dominated by alkalic lavas with high La/Yb and low Zr/Nb, there is an abrupt transition in the 7.7-m interval containing the marginally tholeiitic samples R168, R169, and R171 which have lower La/Yb and higher Zr/Nb (Figure 7); thus these ratios are highly correlated with alkalinity (Figure 8). Slightly lower in the section at 416 m there is an anomalous sample, R208 from flow unit 75, which is tholeiitic in the Na_2O+K_2O versus SiO_2 plot (Figure 1), but unlike other tholeiites it has La/Yb, Zr/Nb (Figure 7), and Sr/Y [*Rhodes*, this
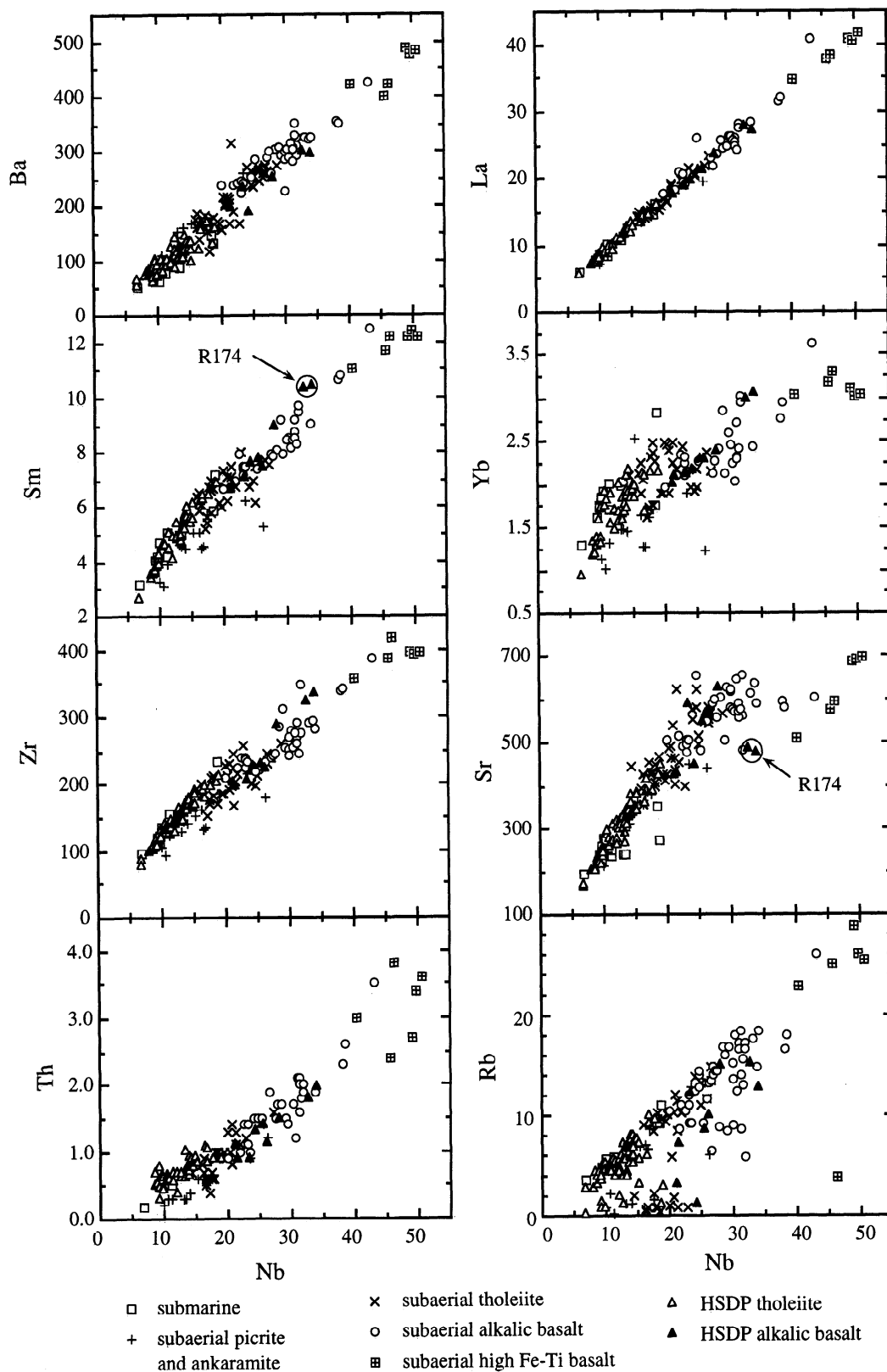
Figure 4. Abundances of incompatible trace elements versus Nb content in Mauna Kea lavas (all in parts per million). The highest abundances are in high Fe-Ti basalts which are relatively young Hamakua lavas. HSDP sample R174 belongs to this group. Samples offset to low Rb also have low K_2O/P_2O_5, and they have lost alkali metals during posteruptive alteration.
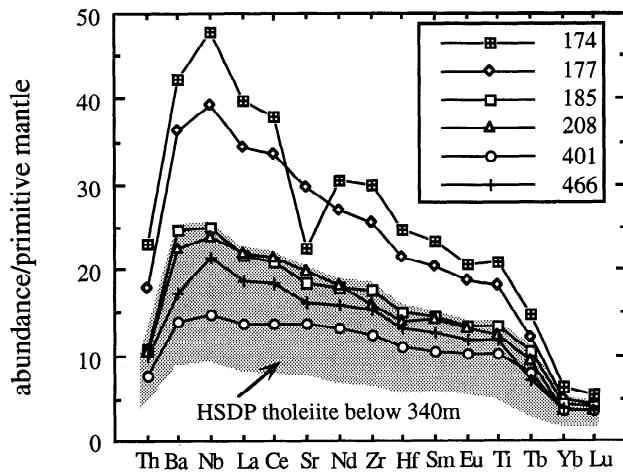
Figure 5. Abundances of incompatible elements in selected HSDP lavas normalized to primitive mantle [*Sun and McDonough*, 1989]. R174 is an Fe-Ti rich basalt that is highly enriched incompatible elements and relatively depleted in Sr. R177 is the most alkalic HSDP lava analyzed. R185 (7.4% MgO) and R208 (10.0% MgO) are examples of the uppermost tholeiitic lavas, and they have crossing REE patterns. R401 is a tholeiitic lava (10.75% MgO) representative of lavas with low abundances of incompatible elements that occurs in the 800 to 950 m interval. R466 is the lowermost Mauna Kea lava; despite its high MgO content (11%) it has higher abundances of incompatible elements than overlying tholeiites with lower MgO contents. Stippled field for lavas below 340 m indicates range for 42 tholeiitic lavas.

issue] which overlap with the overlying alkalic lavas. In relation to other tholeiitic lavas with a similar MgO content, it also has higher Na_2O, K_2O, TiO_2, and P_2O_5 contents [*Rhodes*, this issue] and a crossing chondrite-normalized REE pattern (Figure 5). All other tholeiitic Mauna Kea lavas forming the lower 710 m of the HSDP core define a restricted La/Yb-Zr/Nb field which overlaps with the field for previously studied Hamakua tholeiitic lavas and the dredged submarine lavas from the east rift (Figure 8). From ~420 to 800 m in the core, La/Yb and Zr/Nb do not vary systematically with depth, but samples from ~800 to 950 m define a minimum in La/Yb and a maximum in Zr/Nb (Figure 7).

An important aspect of the La/Yb and Zr/Nb depth profiles is that the oldest six samples, R446 to R466 from flow units 211 through 227 and forming the lower 57 m of the core, have relatively high La/Yb and low Zr/Nb, and they define an inflection in the depth profiles that begins with sample R434 (flow unit 203) at 965 m (Figure 7). This inflection is also clearly demonstrated by the REE data of *Feigenson et al.* [this issue] and the more detailed sampling of *Albarede* [this issue], who analyzed 17 samples from flow units 211 through 227. The data of Albarede (see expanded depth panel of Figure 7a) indicate that this transition to higher La/Yb was episodic with flow units 211 to 218 of olivine and plagioclase-phyric basalt with La/Yb ~6 overlying flow units 219 to 227 of aphyric basalt with La/Yb ~7.

Figure 9 shows how La/Yb has varied during growth of Mauna Kea from ≥400 ka to ~65 ka. The lowest La/Yb ratios are in some of the submarine lavas; however, submarine lava SU-22-64 which erupted distant from the summit [*Yang et al.*, 1994, Figure 1] has a high value of 8.3. Within the tholeiitic part of the HSDP core; i.e., >241 ka, La/Yb varies from 4.9 to 7.0, with R208 at

326 ka having an anomalously high ratio of 8.9. Lavas erupted during the tholeiitic to alkalic transition, ~199 to 241 ka in the HSDP core and in Maulua Gulch, have large variations in La/Yb. Both tholeiitic and alkalic basalts from Waikahalulu gulch have relatively high La/Yb, but the highest values are characteristic of the overlying hawaiites, <65 ka, forming the Laupahoehoe Volcanics.

Discussion

Compositional Effects of Posteruptive Alteration Processes

It is well established that posteruptive processes occurring in high rainfall Hawaiian environments result in preferential loss of K and Rb from subaerially erupted lavas [e.g., *Frey et al.*, 1994]. Obvious manifestations are K_2O/P_2O_5 <1, compared to 1.4 to 2.0 in fresh shield lavas [e.g., *Garcia et al.*, 1989], K/Rb >1000, compared to ~500 in fresh shield lavas [e.g., *Feigenson et al.*, 1983], and poor correlations of K and Rb abundances with abundances of relatively immobile incompatible elements, such as Nb (compare La-Nb and Rb-Nb panels in Figure 4). The east flank of Mauna Kea volcano is a high rainfall region (350-800 cm/yr) and *Frey et al.* [1991] found that 35% of the Hamakua flows from the east flank have K_2O/P_2O_5 <1. Ten of the HSDP samples also have K_2O/P_2O_5 <1, and they have K/Rb ranging from 685 to 3280. Two of these, R331 and R333, are from ~700 m in the core, but the other eight are within the upper 170 m of Mauna Kea lavas (Figure 2c). This result indicates that the uppermost lavas in the HSDP core were erupted in a wet subaerial environment and that they were exposed to surficial alteration processes for a longer time than most of the lower lavas. This inference based on K_2O/P_2O_5 is consistent with ages that indicate an average lava accumulation rate of ~7.8 mm/yr for the lower 641 m of Mauna Kea lavas and only ~0.9 mm/yr for the upper 135 m of Mauna Kea lavas in the HSDP core [*Sharp et al.*, this issue] These accumulation rates are consistent with the most recent estimates for lava supply rate at Mauna Kea which indicate a maximum of 0.06 km^3/yr for tholeiitic lavas forming the main shield with a precipitous decrease to 0.005 km^3/yr for the Hamakua Volcanics, ~250 to 70 ka, and to 0.0004 km^3/yr for the Laupahoehoe Volcanics, <65 ka [*Wolfe et al.*, 1995, Figure 4].

Posteruptive alteration of Hawaiian tholeiites can also lower SiO_2 and increase total iron contents [e.g., *Lipman et al.*, 1990; *Frey et al.*, 1994]. Compared to the general trend of HSDP tholeiitic lavas, three picrites, R189, R193, and R212, from the upper part of the tholeiitic section have anomalously low SiO_2 and high total iron contents (Figures 3a and 3b). These vesicular picrites do not appear to be highly altered in thin section [*Garcia*, this issue], but they have very low K_2O/P_2O_5, <0.7; thus it is likely that their anomalous SiO_2 and total iron contents resulted from posteruptive alteration. Two of these samples, R189 and R212, also have atypically high Th/U (≥3.5 [*Lassiter et al.*, this issue]); in fact, HSDP lavas define an inverse correlation between K_2O/P_2O_5 and Th/U. Loss of U during posteruption alteration of Mauna Kea lavas was previously recognized by *Kennedy et al.* [1991]. Three picrites (R189, R197, R215) from this part of the core have anomalously low Al_2O_3/CaO (Figure 2b). This is unlikely to be an alteration feature since Al_2O_3/CaO is typically increased during alteration [*Lipman et al.*, 1990; *Frey et al.*, 1994], and only one of these picrites (R189) has low K_2O/P_2O_5. Anomalously low Al_2O_3/CaO can result from accumulation of clinopyroxene, but these samples contain less than 0.4 vol % clinopyroxene [*Garcia*, this issue].
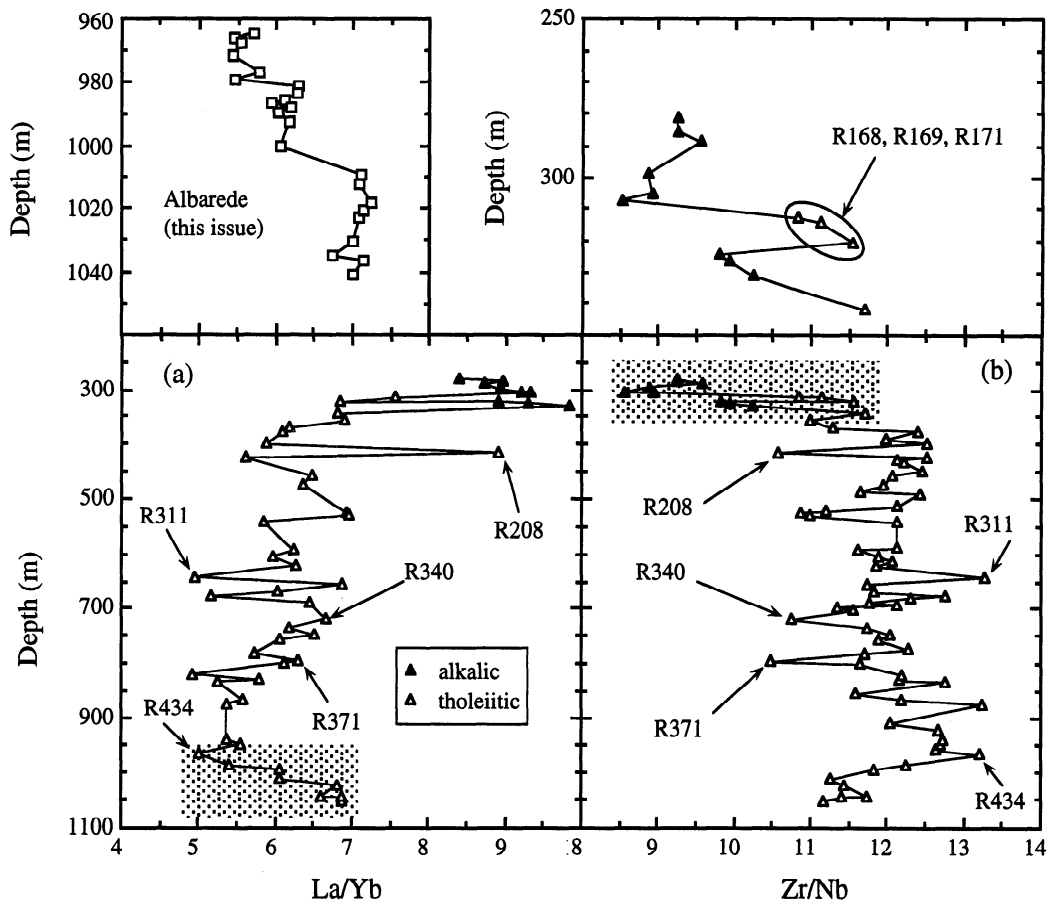
□	submarine	×	subaerial tholeiite	△	HSDP tholeiite
+	subaerial picrite and ankaramite	o	subaerial alkalic basalt	▲	HSDP alkalic basalt
		⊞	subaerial high Fe-Ti basalt		

Figure 6. Incompatible element abundance ratios in Mauna Kea lavas versus Nb content (parts per million). Error bar indicates two standard deviations. In Figure 6b the Th data for HSDP lavas were determined by isotope dilution [*Lassiter et al.*, this issue].

Comparison of Tholeiitic to Alkalic Transition in HSDP Core and Subaerially Exposed Sections

Prior to study of the HSDP core, stratigraphic sections of Mauna Kea lavas with a transition from tholeiitic to alkalic lavas were sampled in three east flank gulches (Laupahoehoe, Kaawalii, and Maulua) and in Waikahalulu gulch on the south slope. Intercalated tholeiitic and alkalic lavas in these sections and the HSDP core have similar isotopic ratios of Sr, Nd, and Pb [*Kennedy et al.*, 1991; *Lassiter et al.*, this issue]. The time span for the alkalic to tholeiitic transition in the HSDP core is defined by an ^{40}Ar-^{39}Ar age of 199±9 ka for alkalic basalt R164, ~19 m below the Mauna Loa-Mauna Kea contact and 241±5 ka for R177, the lowermost alkalic lava in the core [*Sharp et al.*, this

issue]. This age range is consistent with the 237±31 ka K-Ar age of an alkalic basalt from an east flank gulch [*Wolfe et al.*, 1995]. A tholeiitic lava exposed in Waikahalulu gulch high on the south flank of Mauna Kea has a younger K-Ar age of 153±38 ka [*Wolfe et al.*, 1995], but at the 95% confidence level this age overlaps with those reported for the east flank alkalic basalts. Thus the uppermost Mauna Kea lavas in the HSDP core and east flank gulches sample the same time frame of Mauna Kea evolution. This conclusion is strengthened by the occurrence of compositionally distinctive high Fe-Ti basaltic lavas in the east flank gulches and in the HSDP core. Samples from core R174 (flow unit 57) are characterized by moderate MgO contents (5.5%) and high abundances of TiO_2 (4.5%), total iron (Fe_2O_3 ~15%), and P_2O_5 (0.57%) (Figure 3). Such geochemical

Figure 7. La/Yb and Zr/Nb versus depth in the HSDP core. Samples defining inflections are labeled. Stippled fields in Figures 7a and 7b indicate regions with expanded depth scales in the top panels.

Figure 8. La/Yb versus Zr/Nb and alkalinity (see Figure 2 caption) in Mauna Kea lavas. Hamakua tholeiitic lavas from Waikahalulu gulch and HSDP sample R208 have La/Yb and Zr/Nb which overlap with alkalic HSDP lavas, and they are offset to high La/Yb at alkalinity values of 0 to -1. The extremes in La/Yb and Zr/Nb are represented by some submarine lavas and the high Fe-Ti basalt.
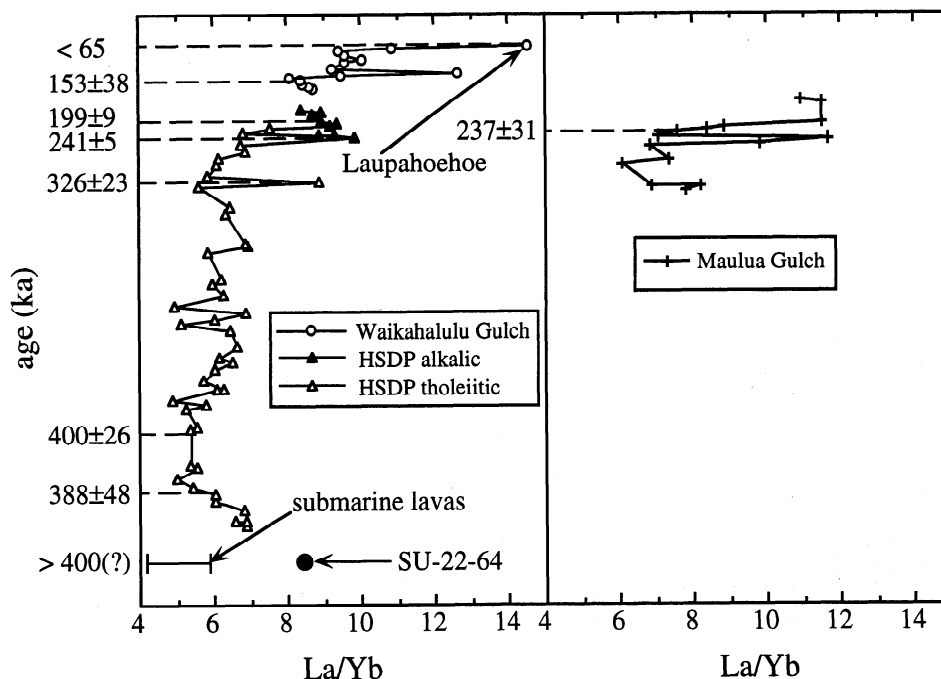
Figure 9. La/Yb as a function of age during growth of Mauna Kea volcano. The vertical scale indicates the stratigraphic position of lavas within the HSDP core, Waikahalulu Gulch and Maulua Gulch with ages from *Wolfe et al.* [1995] and *Sharp et al.* [this issue]. Based on these ages, lavas in Waikahalulu Gulch are inferred to be younger than the uppermost HSDP lavas and lavas in Maulua Gulch are inferred to be contemporaneous with the tholeiitic to alkalic transition in the HSDP core. The undated submarine lavas are inferred to be older than the lowermost HSDP lavas.

characteristics are typical of a distinctive group of Hamakua lavas, high Fe-Ti basalt, that occur in the upper portions of the Hamakua Volcanics; *Wolfe et al.* [1995] found 27 Hamakua lavas with TiO_2 >4.05%, 4.5 to 6% MgO, and K_2O/P_2O_5 >1.6. Although they are geochemically similar, these lavas do not form a single liquid line of descent. For example, at similar MgO contents they range significantly in Al_2O_3/CaO (1.27 to 2.11).

The Fe-Ti rich samples in the HSDP core have relatively high Al_2O_3/CaO, ~1.4 (Figure 2b), within the range found in Hamakua high Fe-Ti lavas. The R174 lavas are not as enriched in incompatible elements as some other high Fe-Ti lavas (Figure 4), but all lavas in this group have a relative deficiency in Sr abundances (Figure 5); consequently, plagioclase was an important fractionating phase during the petrogenesis of these lavas. Supporting evidence for this conclusion is the offset of R174 lavas to low Al_2O_3 (Figure 3). However, neither the R174 lavas (Figure 5) nor the other high Fe-Ti Mauna Kea lavas are depleted in Eu and relatively high oxygen fugacity has been inferred [*Frey et al.*, 1991]. *Frey et al.* [1991] and *Wolfe et al.* [1995] concluded that these Fe-Ti-rich Hamakua lavas formed when pockets of magma became isolated within the crust as magma supply rates decreased toward the end of shield building. As these magmas cooled, gabbroic cumulates segregated and created Fe-Ti-rich residual melts. Because the plagioclase/clinopyroxene ratio in these cumulates varies with pressure, the Al_2O_3/CaO ratio of the residual melts reflects the pressure of crystallization. Using the equations of *Yang et al.* [1996] which relate pressure, temperature and melt composition for melts saturated with olivine, clinopyroxene and plagioclase, we

estimate that many of the Hamakua high Fe-Ti lavas, including R174 samples, formed as residual melts within the upper crust at pressures ranging from 1 atm to ~0.4 GPa (Figure 10). A few high Fe-Ti Hamakua lavas, with lower SiO_2 and higher Al_2O_3/CaO (>1.7), however, require crystal fractionation at higher pressures of 0.6 to 1.2 GPa (Figure 10).

In contrast to the highly evolved high Fe-Ti lavas, which occur in most sections of Hamakua lavas, the basanitoid directly beneath the Fe-Ti-rich unit in the HSDP core (R177 from flow unit 58) has an unusual composition which has not been found in the subaerially exposed sequences. This aphyric lava has high abundances of incompatible elements (Figure 5) and a moderate MgO content (8.21%) but anomalously low SiO_2 (43.7%) and CaO and high Fe_2O_3 (total iron) abundances (Figure 3). An alkalic lava with low SiO_2 (40.6%) and CaO, high total iron, and a moderate MgO content (8.3%) also erupted from the Kanoa cone on the subaerial east flank, northwest of Hilo [*Wolfe et al.*, 1995, Table 19]; in relation to R177 it contains much more TiO_2 (6.1%) and P_2O_5 and has more normative nepheline (12.7%). Both lavas have K_2O/P_2O_5 >1.5, and there is no evidence that these unusual compositions result from alteration. No radiogenic isotope data are available for these highly alkalic lavas. Consequently, it is unknown whether they were derived from a distinctive source composition or if they formed by unusually low extents of melting. The compositional contrast between alkalic lava R177 at 331.6 m and the underlying tholeiitic lava R180 in flow unit 59 at 342 m (Table 1 of this paper and *Rhodes* [this issue]) shows the compositional diversity of nearly coeval magmas that erupted at Mauna Kea at ~240 ka.
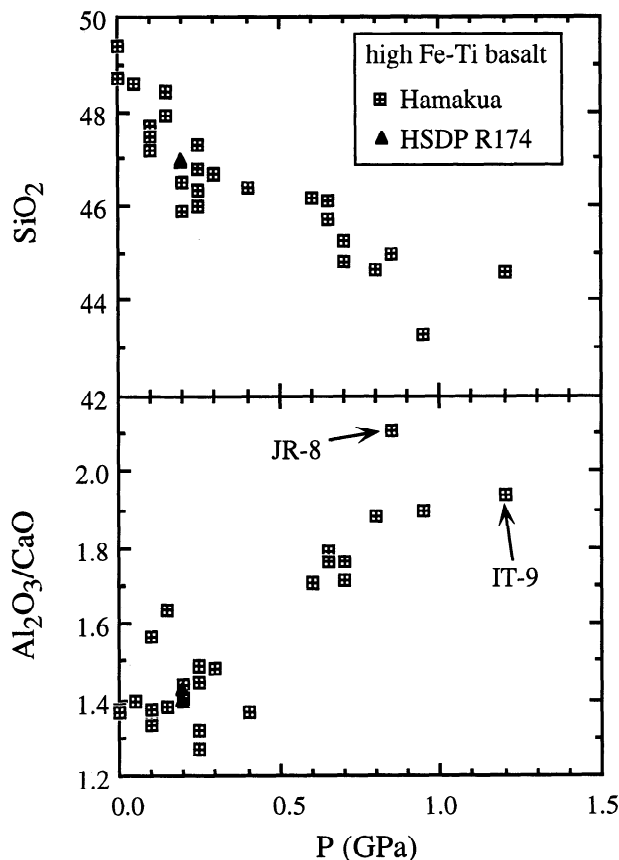
Figure 10. Al_2O_3/CaO and SiO_2 contents (in weight percent) in high Fe-Ti Hamakua lavas versus estimated pressures [*Yang et al.*, 1996]. HSDP lava R174 belongs to this group. Hamakua data are from *Frey et al.* [1991] and *Wolfe et al.* [1995] with sample numbers for two samples equilibrated at high pressure.

Petrogenetic Inferences Resulting From Systematic Changes in Magma Composition as a Function of Depth in the HSDP Core

Role of crustal processes. The compositions of HSDP lavas were affected by mineral-melt segregation within the crust. The alkalic lavas with low MgO contents, especially the Fe-Ti-rich R174 samples, formed as residual melts after extensive crystal fractionation. Below 368 m in the core, MgO-rich picrites are abundant. The MgO content of Hawaiian primary magmas is a constraint on the melting processes involved in plume-related volcanism. *Wright* [1984] proposed MgO contents of 20 to 22% for primary Hawaiian magmas. Also glasses representing quenched melts containing ~15% MgO have been found on the submarine flanks of Kilauea [*Clague et al.*, 1991]. Melts with compositions similar to these glasses are saturated only with olivine and orthopyroxene at upper mantle pressures and volatile-free conditions [*Eggins*, 1992a; *Wagner and Grove*, 1992]. This inference conflicts with evidence based on heavy REE abundances in Hawaiian shield lavas that garnet was a significant residual phase [e.g., *Hofmann et al.*, 1984; *Eggins*, 1992b; *Frey et al.*, 1994; *Feigenson et al.*, this issue]. A possible resolution of this paradox is that Hawaiian primary magmas contain more than 15% MgO [*Eggins*, 1992a; *Garcia et al.*, 1995]. Thus it is

important to assess if any of the HSDP lavas with high-MgO contents are representative of high-MgO melts.

Yang et al. [1994] used MgO-Ni abundance trends to show that dredged Mauna Kea shield lavas contain accumulated olivine; consequently, these lavas are not representative of high MgO melts. If Ni partition coefficients for olivine/melt from *Hart and Davis* [1978] or *Kinzler et al.* [1990] are used, the same conclusion is valid for MgO-rich HSDP lavas; that is, the near-linear MgO-Ni trend from ~12 to 28% MgO can be explained by addition of Fo_{86} olivine to lavas, such as R463, with ~12% MgO (Figure 11). However, if a lower Ni partition coefficent is used [*Mörse et al.*, 1991], it is difficult to distinguish between olivine accumulation and fractionation (Figure 11). Although there is ambiguity in interpreting the MgO-Ni trends, *Baker et al.* [this issue] and *Garcia* [this issue] conclude that primary magmas with 15-17% MgO are required to create the forsterite-rich olivines in HSDP lavas.

Mantle processes: Variable extents of melting. Earlier we noted the systematic variations of La/Yb and Zr/Nb with depth in the HSDP core; in particular, the relative enrichment of the highly incompatible elements La and Nb in the uppermost alkalic Mauna Kea lavas and in tholeiitic lavas from the lowermost 57 m of core (Figure 7). These incompatible element abundance ratios are not very sensitive to postmelting processes such as mineral accumulation and segregation; consequently, we infer that significant changes in primary magma composition occurred during the ~200-kyr interval represented by the HSDP core. In order to evaluate variations in extent of melting and depth of melt segregation during this time period, it is necessary to infer primary magma compositions from the compositions of HSDP lavas. Whole rock compositions cannot be used directly because (1) the whole rocks may not be representative of melts and (2) none of the HSDP lavas are crystallized primary magmas [*Baker et al.*, this issue; *Garcia*, this issue]. In order to infer compositions of the primary magmas represented in the HSDP core, we focus on the 24 HSDP lavas which have <8% phenocrysts, K_2O/P_2O_5 > 1.4, and $\geq 7.4\%$ MgO; this subset includes 2 alkalic and 22 tholeiitic lavas. Based on these criteria and the absence of correlations between abundance ratios sensitive to fractionation of plagioclase and clinopyroxene, such as Al_2O_3/CaO, Sc/Y, and Sr/Nd, we assume that the compositions of these 24 lavas are representative of melts whose compositions were largely controlled by olivine fractionation. Primary magma compositions for these lavas were estimated by adjusting FeO contents to 85% of the total iron content and then adding equilibrium olivine in 1% increments to the measured lava compositions until the MgO content is 16%. This MgO content is typical of primary magmas inferred for other Hawaiian shields [e.g., *Clague et al.*, 1991; *Chen*, 1993; *Garcia et al.*, 1995]. Our following discussion is not sensitive to this choice of MgO content for primary magmas, but at 16% MgO these HSDP lavas are in equilibrium with olivine of $Fo = 90.3\pm0.4$ which is similar to the maximum Fo contents found in HSDP picritic lavas [*Baker et al.*, this issue; *Garcia*, this issue].

The inferred primary magma compositions show systematic compositional variations with depth in the HSDP core. For example, incompatible elements and oxides, such as Nb, Zr, TiO_2, P_2O_5, and Na_2O, have higher abundances in the upper 50 m of the Mauna Kea core (Figure 12). In addition, abundances of Nb, Zr, TiO_2, and P_2O_5 reach minima at depths of 800 to 950 m and increase systematically from 950 m to the bottom of the core
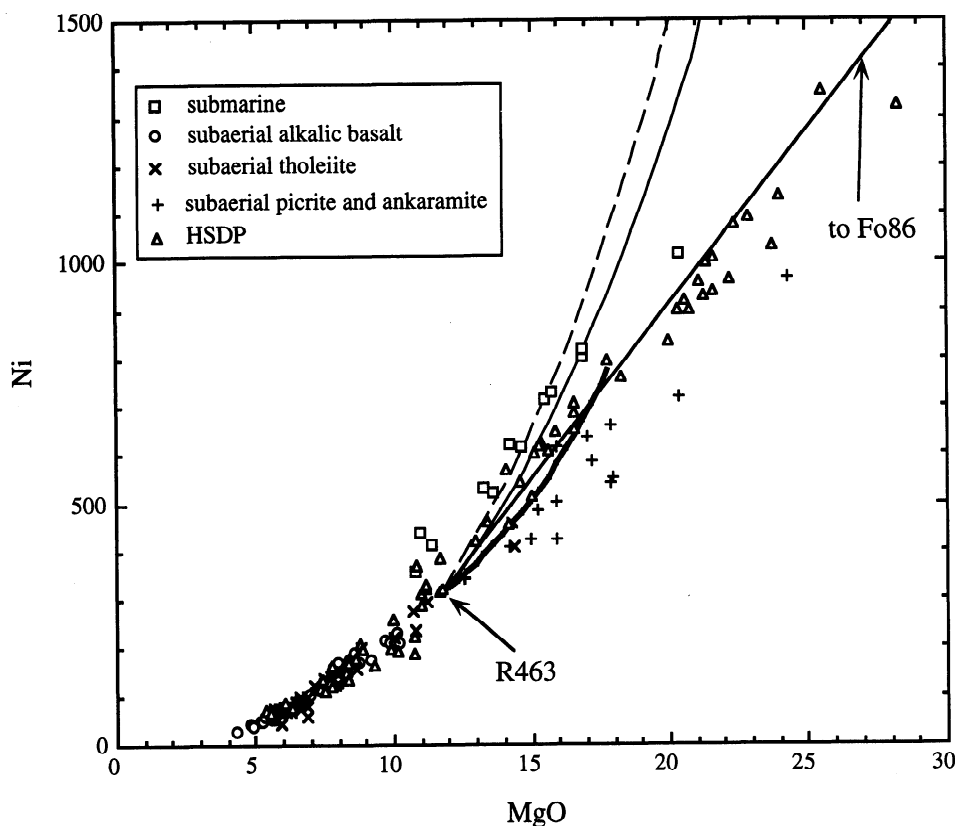
Figure 11. Ni (in parts per million) versus MgO content (in weight percent) for HSDP, submarine, and subaerially exposed Mauna Kea lavas. The curves are for olivine fractionation and were calculated by adding 1% increments of olivine to the composition of lava R463, a MgO-rich lava with ~6% olivine [*Garcia*, this issue]. Olivine Fe/Mg ratios are based on a K_D of 0.3 and Ni contents were determined following *Hart and Davis* [1978], dashed line, or *Kinzler et al.* (1990), thin solid line; at 13% MgO the Ni partition coefficients are 8 and 7, respectively. The thick solid curve emanating from R463 shows the effects of a constant but lower Ni partition of 6 which is consistent with the results of *Morse et al.* [1991]. The straight line is for addition of Fo_{86} olivine to R463.

(Figure 12). Abundances of these elements in the lowermost tholeiitic lavas, however, are lower than those of the alkalic lavas in the upper part of the Mauna Kea section. The maximum/minimum abundance ratios for the inferred primary magmas are Nb = 2.5, La = 2.5, P_2O_5 = 2.2, Zr = 2.0, TiO_2 = 1.7 and Na_2O = 1.4. This ordering of elements corresponds to the order of increasing compatibility during partial melting of peridotite [e.g., *Sun and McDonough*, 1989].

We infer that the systematic variation in abundances of incompatible elements with depth corresponds to changes in extent of melting as a function of time. This inference is particularly plausible for the upper 343 m of Mauna Kea lavas which have very similar isotopic ratios of Sr, Nd, and Pb [*Lassiter et al.*, this issue]. Based on differences in abundances of Nb at 16% MgO, the extent of melting varied by a factor of 2.1, in the 343-m interval of Mauna Kea lavas from flow unit 45 to flow unit 120. The isotopic homogeneity of the tholeiitic to alkalic transition in the HSDP core [*Lassiter et al.*, this issue] is also characteristic of the stratigraphic sections from the east flank gulches [*Kennedy et al.*, 1991]. At the same stage of volcano growth, intercalated tholeiitic and alkalic basalts with similar isotopic ratios also erupted at Haleakala [*Chen et al.*, 1991] and Kohala [*Hofmann et al.*, 1987; *Lanphere and Frey*, 1987]. Apparently, at each of these volcanoes, both basalt types were

derived from a common source by significantly different extents of melting, approximately a factor of 2 for Mauna Kea [this paper; *Frey et al.*, 1991; *Feigenson et al.*, this issue]. The major conclusion is that as a Hawaiian volcano moves away from the mantle plume and magma production decreases, it is possible to extract and erupt magmas of similar age that were formed by very different extents of melting of a common source.

In the lowermost 433 m of the HSDP core, there are small but significant changes in isotopic ratios of Sr, Nd, and Pb [*Lassiter et al.*, this issue]; consequently, the source composition may also have been variable. These isotopic variations, however, are not strongly correlated with compositional changes in the inferred primary magmas. Therefore we assume that differences in incompatible element abundances and ratios at 16% MgO in the lower 433 m of core are also indicative of variations in extent of melting. With this assumption, five of the six analyzed tholeiites from ~800 m to 950 m in the core formed by relatively higher extents of melting, a factor of 2.5 larger than basanitoid R177 from flow unit 58 at 332 m. A surprising result is that there is a trend to higher incompatible element contents, established by the five samples from units 218 to 227 at the bottom of the core (R452, R457, R463, R464, and R466 from 1009.5 to 1052.4 m); hence these lavas were formed by lower extents of melting. As this trend is apparent in measured La/Yb and Zr/Nb (Figure 7)
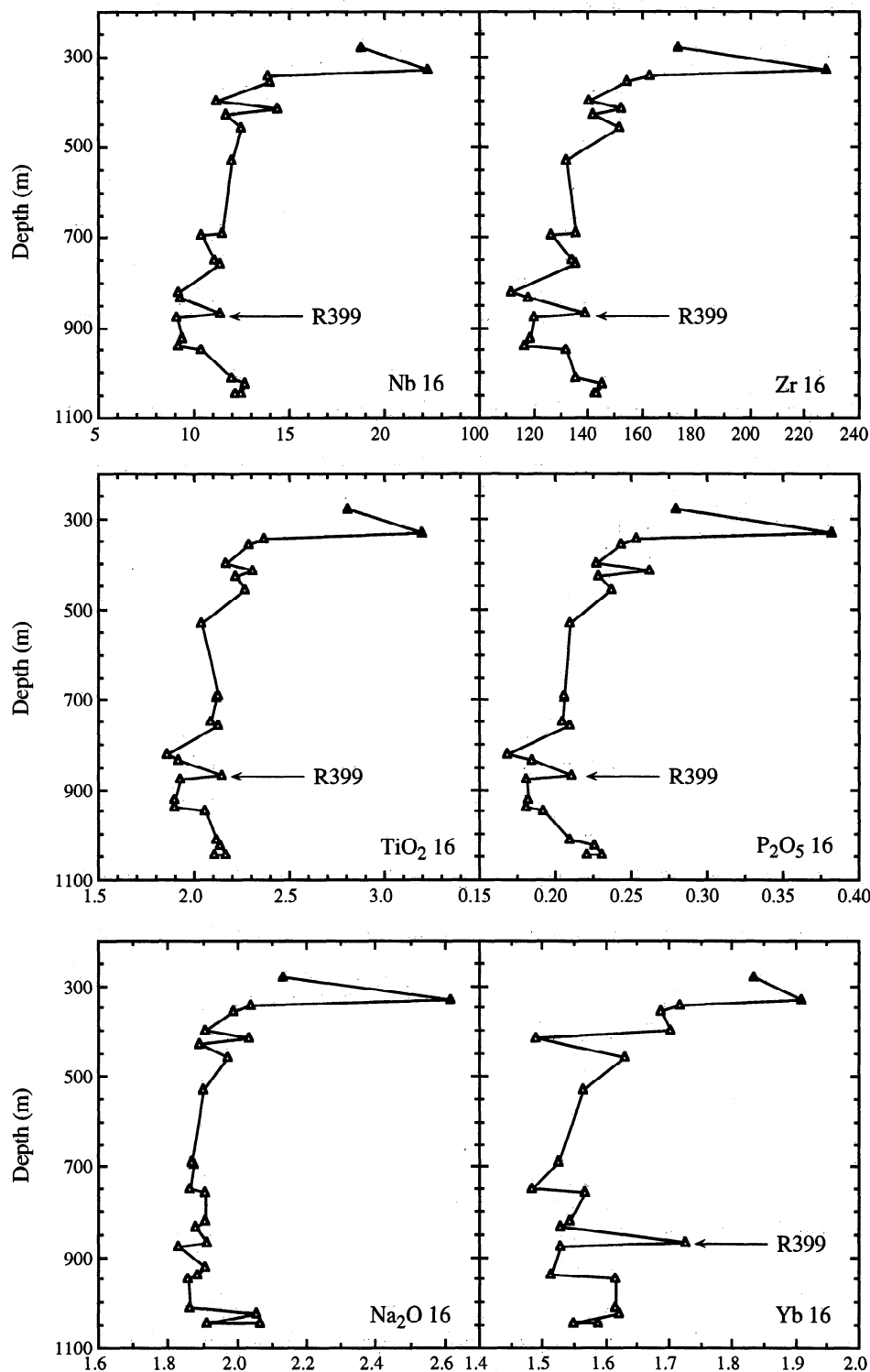
Figure 12. Abundances of incompatible elements (in parts per million) and oxides (in weight percent) in estimated primary magma compositions (16% MgO) for 24 HSDP lavas as a function of height in the HSDP core. Primary magma compositions were determined by adding equilibrium olivine in 1% increments until MgO contents were 16%. Solid symbols indicate alkalic lavas.

and in calculated abundances of incompatible elements at 16% MgO (Figure 12), we are confident that these lavas reflect a significant change in the melting process.

In summary, a complex variation in extent of melting is recorded over the approximately 200-kyr interval represented by

Mauna Kea lavas in the HSDP core. Basanitoid R177 at 332 m formed by the lowest extent of melting. From this level to ~800-950 m, the tholeiitic HSDP lavas record a slow increase in degree of melting culminating with a maximum recorded by lavas in the 800-950 m region. Below 950 m, there is a reversal in trend, and
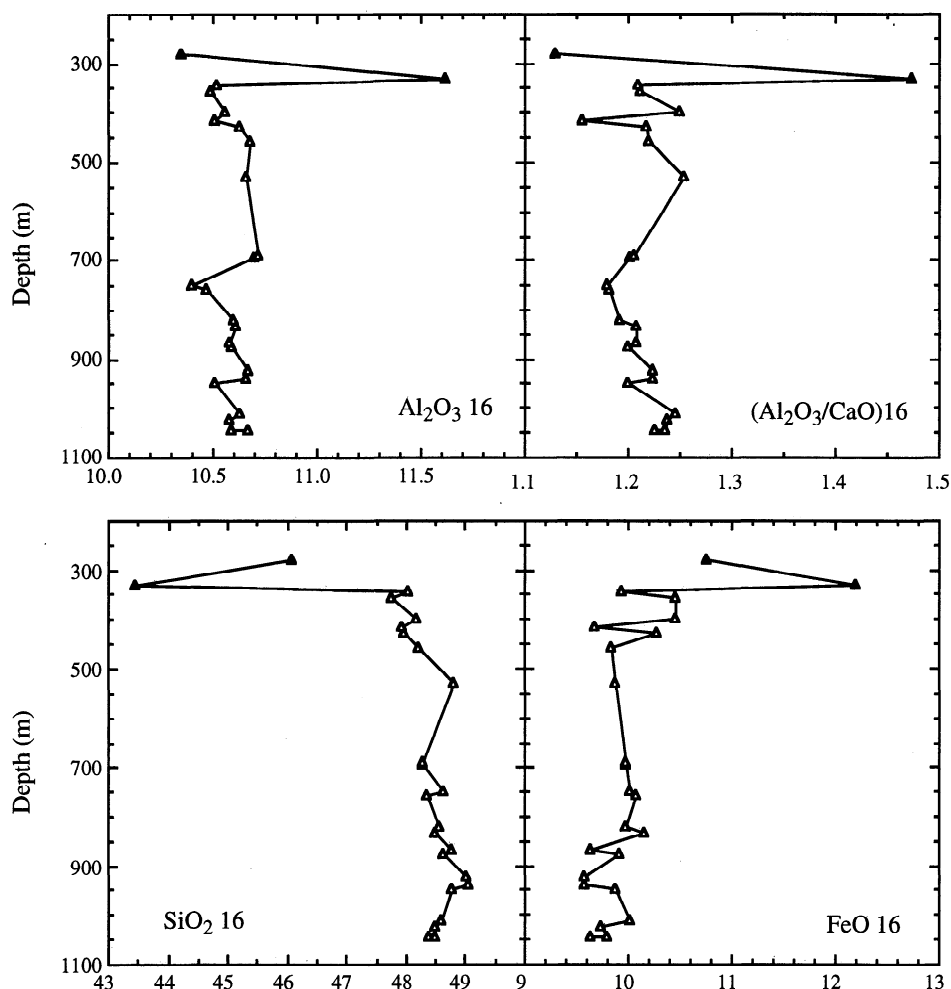
Figure 13. Abundances of Al_2O_3, SiO_2, and FeO (in weight percent) and Al_2O_3/CaO ratio in estimated primary magma compositions (16% MgO) for 24 HSDP lavas as a function of height in the HSDP core. See text and Figure 12 caption for procedures used to calculate primary magma compositions. Solid symbols indicate alkalic lavas.

lavas within the lowermost 100 m define a trend of decreasing extent of melting with increasing depth. As a result, tholeiitic lavas at 400 and 1050 m formed by similar extents of melting.

Mantle processes: Constraints on residual mineralogy. In contrast to the systematic variations in incompatible element abundances with depth in the core, abundances of Al_2O_3 and the Al_2O_3/CaO ratio in the inferred primary magmas show no systematic trend with depth (Figure 13). Except for basanitoid R177 which has >11% Al_2O_3, the other 23 inferred primary compositions range in Al_2O_3 only from 10.4 to 10.7%. The Al_2O_3/CaO ratio of these 23 samples ranges from 1.13 to 1.26. The uniformity of Al_2O_3 in lavas derived by variable extents of melting suggests control by an aluminous residual phase, such as garnet, during the melting process. Based on geophysical constraints, Hawaiian shield lavas segregate at depths where garnet is an important residual phase [*Watson and McKenzie*, 1991]. This conclusion is consistent with the near constancy of Y and heavy REE abundances in Hawaiian shield lavas derived by variable extents of melting [e.g., *Hofmann et al.*, 1984; *Frey et al.*, 1994]. Within the HSDP core, primary magmas below 400 m have a narrow range, ~1.5 to 1.6 ppm, in Yb (sample R399 is an exception), but the alkalic and tholeiitic lavas from the uppermost Mauna Kea lavas have higher Yb contents of ~1.7 to 1.9 ppm Yb

(Figure 12). If these uppermost lavas were derived from a source with similar Yb content by lower extents of melting, as inferred from their Nb contents (Figure 12), the bulk solid/melt partition coefficient for Yb was slightly less than unity. For a Yb garnet/melt partition coefficient of 5, this result requires less than 20% garnet in the residue.

Mantle processes: Constraints on depth of melt segregation. The depth profiles for SiO_2 and FeO abundances in the inferred primary magma compositions differ from those for Al_2O_3, CaO, and incompatible elements. Compared to tholeiitic lavas in the core, the alkalic lavas were derived from primary magmas with relatively higher FeO and lower SiO_2 contents (Figure 13). Abundances of these oxides in melts derived from spinel peridotite and probably garnet peridotite are sensitive to the pressure of melt segregation; as pressure increases, abundances of SiO_2 decrease and of FeO increase (e.g., see review by *Langmuir et al.* [1992], and *Kinzler and Grove* [1992], *Hirose and Kushiro* [1993], *Takahashi et al.* [1993], and *Walter and Presnall* [1994]). Although abundances of SiO_2 and FeO are also dependent on extent of melting, from 2 to 3 GPa their abundances are not very sensitive to extent of melting [*Hirose and Kushiro*, 1993]. Therefore we conclude that the combination of lower SiO_2 and higher FeO in the alkalic lavas reflects melt segregation at higher

pressure. Within the tholeiitic part of the HSDP core, systematic variations in SiO_2 and FeO contents are more subdued. However, in the interval from 350 m to 950 m, the lowest SiO_2 (~48%) and highest FeO (>10.2%) contents are in uppermost tholeiitic lavas (Figure 13). In addition, the six lowermost lavas in the core which define a trend of increasing abundances of incompatible elements (Figure 12) also define a trend of decreasing SiO_2 content (Figure 13). Thus HSDP lavas define a trend of decreasing extents of melting with increasing pressures of melt segregation.

Comparison of Inferred Primary Magmas Compositions for HSDP Core and Subaerially Exposed Lavas

Based on lava compositions and ages, the uppermost 50 m of Mauna Kea lavas in the HSDP core overlap with the lavas subaerially exposed low on the east flank of Mauna Kea. The lowermost lavas in the HSDP core may be comparable in age to the submarine lavas dredged from the east rift. Although these submarine lavas have not been dated, a gross estimate of 400 ka was made by *Wolfe et al.* [1995], who used a subsidence rate of 2.6 mm/yr and an inference based on vesicularity that some of the submarine lavas have subsided 1000 m [*Moore and Peck*, 1966]. This age is similar to the 400±26 ka reported for sample R423 from near the bottom of the HSDP core [*Sharp et al.*, this issue]. Thus the HSDP core contains an extended record of tholeiitic volcanism which fills the time gap between the east flank gulches and the dredged submarine lavas.

Following the process used for inferring primary magma compositions of HSDP lavas, we also calculated primary magma compositions for 11 tholeiitic and 18 alkalic lavas from subaerial exposures on Mauna Kea volcano and the most MgO-rich (6.9%) submarine glass (SU-46 of *Yang et al.* [1994]). All of these lavas have <5% phenocrysts and are unaltered with K_2O/P_2O_5 >1.4, but in order to have a suitable data base, we lowered the MgO limit to 6.8%. The inferred primary magma compositions for HSDP and subaerially exposed lavas show inverse correlations between SiO_2 versus FeO and SiO_2 versus Nb (Figure 14). Inverse correlations between abundances of major oxides and SiO_2 content can result from the necessity for oxide abundances to sum to 100%. There is only a poor inverse correlation between Al_2O_3 and SiO_2 abundance, especially among the HSDP lavas (Figure 14); thus we conclude that the inverse $FeO-SiO_2$ trend has petrogenetic significance. The relatively young alkalic lavas have the highest Nb and FeO contents and lowest SiO_2 contents. Following ideas presented earlier, we conclude that the compositions of Mauna Kea lavas, in general, show that pressures of melt segregation and extent of melting are inversely related. Compared to subaerially exposed lavas, the tholeiitic HSDP lavas and the submarine sample formed at lower pressures by larger extents of melting, with the highest extents of melting recorded by lavas in the 800-950 m interval of the HSDP core and the submarine glass. Among the subaerially exposed lavas, the alkalic lavas reflect the lowest extent of melting and highest pressures of melt segregation.

In summary, Mauna Kea lavas show an overall trend for the pressure of melt segregation to increase and extent of melting to decrease as the volcano aged. Superimposed on this long-term trend there are short-term changes in extent of melting within the uppermost 50 m of Mauna Kea lavas and a reversal of the trend near the bottom of the HSDP core. Although no age is available, submarine sample SU22-64, which is transitional in composition [*Yang et al.*, 1994] and has anomalously high La/Yb (Figure 9), may also be an anomaly in the long-term trend.
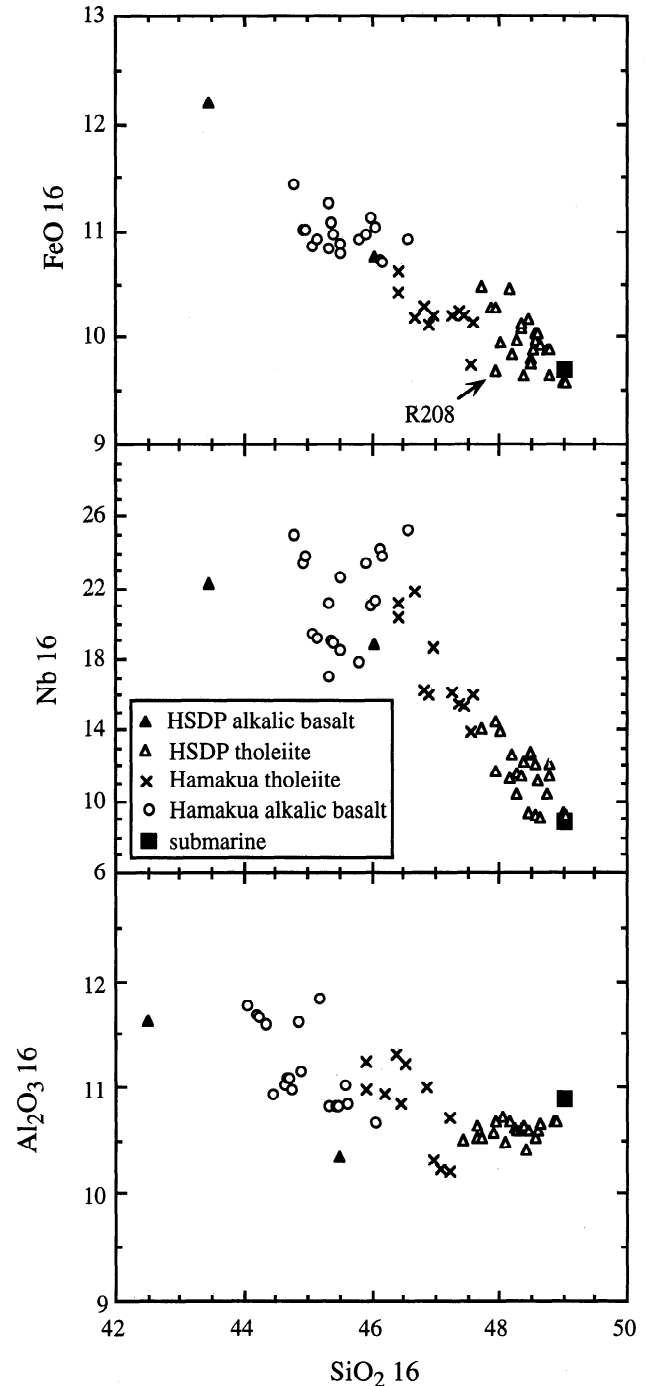

Figure 14. Abundances of FeO, Nb, and Al_2O_3 versus SiO_2 content (all in weight percent except for Nb in parts per million) in estimated primary magma compositions (16% MgO) for Mauna Kea lavas. See text and Figure 12 caption for procedures used to calculate primary magma compositions.

In a comparison of alkalic and tholeiitic Hawaiian lavas representing different growth stages of several Hawaiian volcanoes, *Langmuir et al.* [1992, Figure 65] also concluded that extent of melting is inversely related to pressure of melt segregation. A similar trend is also characteristic of lavas from the Galapagos [*Geist*, 1992] and Main Lava Series from Skye, Scotland [*Scarrow and Cox*, 1995]. At each of these localities the correlations between abundances of FeO, SiO_2, and incompatible
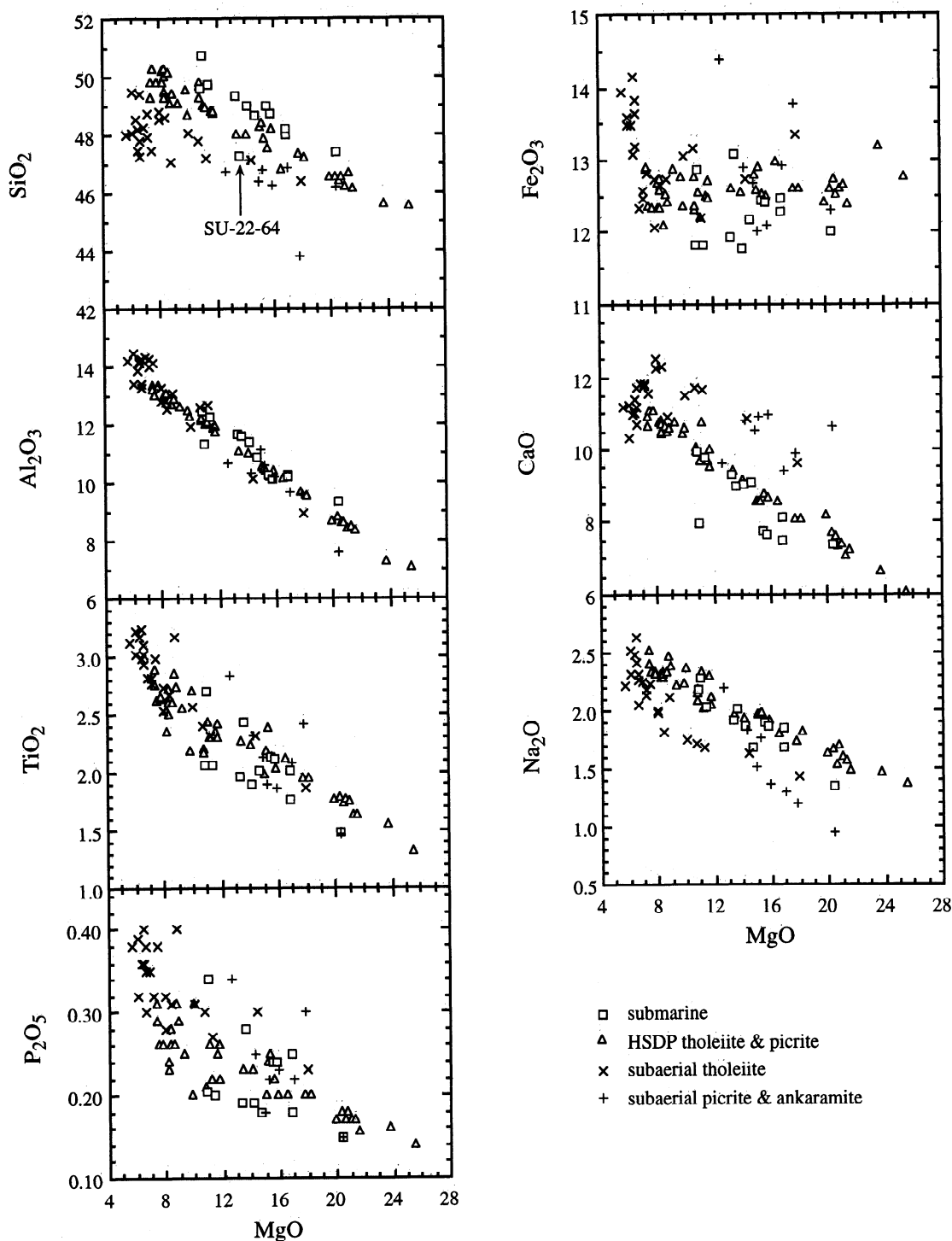
Figure 15. Abundances of oxides versus MgO content (all in weight percent) in tholeiites, picrites, and ankaramites from Mauna Kea volcano. Altered samples with K_2O/P_2O_5 <1 are not plotted. On average, in the range of MgO = 10 to 20%, the lava groups, submarine-HSDP- subaerial, correspond to decreasing SiO_2, higher Fe_2O_3, (total iron) and higher CaO.

elements, such as Nb, result largely from comparisons of alkalic and tholeiitic basalts. Among Mauna Kea lavas, however, much of the systematic variation in Figure 14 is defined by tholeiitic lavas. Thus it is of interest to evaluate in more detail the temporal compositional variations of tholeiitic Mauna Kea lavas.

In the following discussion we use compositional data for all HSDP and subaerial and submarine Mauna Kea lavas that plot within the tholeiitic field (Figure 1b). Previously, we used

calculated primary magma compositions to infer temporal changes in the mantle melting processes. An alternative approach used by *Frey and Rhodes* [1993] is to compare suites of lavas on MgO variation diagrams. This alternative enables use of the entire data set and avoids assumptions inherent in estimating primary magma compositions. It is, however, viable only when the data define coherent MgO variation trends.

Abundances of Al_2O_3 and the moderately incompatible oxides,

TiO_2 and P_2O_5, define overlapping fields for the tholeiitic basalts from the HSDP core, the submarine east rift, and subaerially erupted lavas (Figure 15). In contrast, Mauna Kea tholeiites from these locations are offset in a plot of MgO versus SiO_2; i.e., if lavas with 10 to 20% MgO are grouped as submarine, HSDP, and subaerially exposed suites, this is, in general, a sequence of decreasing SiO_2 content. Although there is scatter and overlap, this is also a sequence of increasing CaO and Fe_2O_3 (total iron).

What is the cause of these temporal variations in major element abundances? Two possibilities are differences in source composition or, as discussed earlier, differences in pressure of melt segregation. The former is likely to be accompanied by differences in radiogenic isotope ratios. Indeed, within the HSDP core the highest $^{87}Sr/^{86}Sr$ and lowest $^{143}Nd/^{144}Nd$ occur in the lower parts of the core, and some submarine lavas extend to even higher $^{87}Sr/^{86}Sr$ and lower $^{143}Nd/^{144}Nd$ [*Yang et al.*, 1994; *Lassiter et al.*, this issue, Figure 2]. Nevertheless, there is no correlation between these isotopic ratios and SiO_2/FeO at a given MgO content. Moreover, *Frey and Rhodes* [1993] found no correlation between intershield differences in major element abundances and isotopic ratios of Sr, Nd, and Pb. Therefore we assume a uniform major element composition for the source of all Mauna Kea tholeiites. Following our earlier discussion, the trends to lower SiO_2 and higher total iron contents from submarine east rift to HSDP core to subaerially exposed lavas can be interpreted as indicating increasing pressures of melt segregation. This is also a sequence of increasing mean La/Yb and decreasing mean Zr/Nb (Figures 8 and 9) which is consistent with a decrease in extent of melting. If the submarine lavas are older than HSDP samples, the trend is for pressure of melt segregation to increase and extent of melting to decrease with decreasing age. This trend is the same as that inferred from the calculated primary magma compositions.

The increase in CaO content at a given MgO content from submarine east rift to HSDP to subaerially exposed lavas is not easily explained. If decreasing SiO_2 content reflects increasing pressure, it follows that CaO content increases with increasing pressure of melt segregation. Existing experimental data for melting of spinel peridotite provide no supporting evidence for this inference [e.g., *Kinzler and Grove*, 1992; *Hirose and Kushiro*, 1993]. Abundances of SiO_2 and CaO are also discriminants between some Hawaiian shields [see *Frey et al.*, 1994, Figure 11, *Frey and Rhodes*, 1993, Figure 2]. *Frey and Rhodes* [1993] speculated that variable CaO contents indicate an important role for CO_2 during partial melting.

Implications For How the Hawaiian Plume "Works"

Studies of Hawaiian tholeiitic basalts show that (1) they retain information about the extent of melting and depths of melt segregation, and (2) these parameters vary systematically with time and location relative to the plume axis [e.g., *Frey and Rhodes*, 1993; *Hauri et al.*, this issue; *Lassiter et al.*, this issue]. For example, the intershield compositional differences between volcanoes formed along the spatial Loa (e.g., Mauna Loa and Hualalai) and Kea trends (e.g., Kilauea, Mauna Kea, and Kohala) are consistent with derivation of Loa lavas by higher extents of melting with melt segregation at lower pressures. In the context of a plume model a plausible interpretation is that the Loa volcanoes formed directly over the hot plume axis, whereas the Kea volcanoes form above the plume periphery from ascending mantle that is cooler and whose ascent is modified by plate motion.

The HSDP core shows the geochemical evolution of individual volcanoes, from ~10 to 100 ka for Mauna Loa and ~200 to 400 ka for Mauna Kea. By comparing the geochemical characteristics of Mauna Kea lavas in the HSDP core with results from subaerially exposed and submarine Mauna Kea lavas we infer the following trends as Mauna Kea moved away from the plume.

1. Among Mauna Kea lavas, the lowest $^{143}Nd/^{144}Nd$ are in some of the submarine lavas and the lowermost flows in the HSDP core [*Yang et al.*, 1994; *Lassiter et al.*, this issue]. These lavas, ~400 ka, contain the largest proportion of an enriched (plume?) component.

2. As eruption age decreased from ~400 to 240 ka there was a general long-term trend for tholeiitic magmas to segregate at higher pressure and form by lower extents of melting. This inverse trend between extent of melting and pressure of melt segregation is analogous to that which distinguishes Loa and Kea volcanoes. Although this trend has not been previously documented for the shield stage of Hawaiian volcanoes, a similar trend can be inferred for Haleakala, another Kea trend volcano. That is, at a given MgO content, submarine tholeiites from Haleakala have higher SiO_2 and CaO contents and lower total iron, TiO_2, and P_2O_5 contents than subaerial Haleakala tholeiites [see *Chen et al.*, 1991, Figure 4]. If these submarine Haleakala lavas are older than the subaerial lavas, there was also a trend for pressure of melt segregation to increase and extent of melting to decrease as the Haleakala shield-stage ended.

3. At ~330 ka, magma supply rate decreased precipitously [*Sharp et al.*, this issue].

4. From ~240 to 200 ka, coeval tholeiitic and alkalic basalts with similar radiogenic isotopic ratios were erupted. Short-term variations in extent of melting are required.

5. From ~240 to 70 ka, shallow crustal level magma reservoirs crystallized, and some alkalic basaltic magmas ponded at various depths within the crust and upper mantle where they cooled, crystallized gabbroic cumulates, and formed residual Fe-Ti rich lavas.

6. Basaltic magmatism ceased at ~70 ka, and pockets of alkalic basalt stagnated near the crust-mantle boundary. With cooling, a clinopyroxene-rich assemblage containing Fe-Ti oxides crystallized and segregated, thereby creating low-density residual melts, the hawaiites of the Laupahoehoe Volcanics, which erupted from ~65 to 4 ka.

References

Albarède, F., High-resolution geochemical stratigraphy of Mauna Kea flows from the Hawaii Scientific Drilling Project core, *J. Geophys. Res.*, this issue.

Baker, M. B., S. Alves, and E. M. Stolper, Petrography and petrology of the Hawaii Scientific Drilling Project lavas: Inferences from olivine phenocryst abundances and compositions, *J. Geophys. Res.*, this issue.

Chen, C.-Y., High-magnesium primary magmas from Haleakala volcano, east Maui: Petrography, nickel, and major element constraints, *J. Volcanol. Geotherm. Res.*, 55, 143-153, 1993.

Chen, C.-Y., and F. A. Frey, Trace element and isotopic geochemistry of lavas from Haleakala volcano, east Maui, Hawaii: Implications for the origin of Hawaiian lavas, *J. Geophys. Res.*, 90, 8743-8768, 1985.

Chen, C.-Y., F. A. Frey, and M. O. Garcia, Evolution of alkalic lavas at Haleakala Volcano, east Maui, Hawaii: Major, trace element and isotopic constraints, *Contrib. Mineral. Petrol.*, 105, 197-218, 1990.

Chen, C.-Y., F. A. Frey, M. O. Garcia, and B. Dalrymple, The tholeiite to alkalic basalt transition at Haleakala volcano, Maui, Hawaii, *Contrib. Mineral. Petrol.*, *106*, 183-200, 1991.

Chen, C.-Y., F. A. Frey, J. M. Rhodes, and R. M. Easton, Temporal geochemical evolution of Kilauea volcano: Comparison of Hilina and Puna basalt, in *Earth Processes: Reading the Isotopic Code, Geophys. Monogr. Ser.*, vol. 95, edited by A. Basu and S.R. Hart, AGU, Washington, D.C., in press, 1996.

Clague, D. A., and G. B. Dalrymple, The Hawaiian-Emperor volcanic chain, 1, Geologic evolution, *U.S. Geol. Surv. Prof. Pap.*, 1350, 5-54, 1987.

Clague, D. A., W. S. Weber, and J. E. Dixon, Picritic glasses from Hawaii, *Nature*, *353*, 553-556, 1991.

Eggins, S. M., Petrogenesis of Hawaiian tholeiites, 1, Phase equilibria constraints, *Contrib. Mineral. Petrol.*, *110*, 387-397, 1992a.

Eggins, S. M., Petrogenesis of Hawaiian tholeiites, 2, Aspects of dynamic melt segregation, *Contrib. Mineral. Petrol.*, *110*, 398-410, 1992b.

Feigenson, M. D., A. W. Hofmann, and F. J. Spera, Case studies on the origin of basalt, II, The transition from tholeiitic to alkalic volcanism on Kohala volcano, Hawaii, *Contrib. Mineral. Petrol.*, *84*, 390-405, 1983.

Feigenson, M. D., L. C. Patino, and M. J. Carr, Constraints on partial melting imposed by rare earth element variations in Mauna Kea basalts, *J. Geophys. Res.*, this volume, 1995.

Fodor, R. V., and H. J. Vandermeyden, Petrology of gabbroic xenoliths from Mauna Kea volcano, Hawaii, *J. Geophys. Res.*, *93*, 4435-4452, 1988.

Frey, F. A., and J. M. Rhodes, Intershield geochemical differences among Hawaiian volcanoes: Implications for source compositions, melting process and magma ascent paths, *Philos. Trans. R. Soc. London A*, *342*, 121-136, 1993.

Frey, F. A., W. S. Wise, M. O. Garcia, H. West, S. T. Kwon, and A. Kennedy, Evolution of Mauna Kea volcano, Hawaii: The transition from shield building to the alkalic cap stage, *J. Geophys. Res.*, *95*, 1271-1300, 1990.

Frey, F. A., M. O. Garcia, W. S. Wise, A. Kennedy, P. Gurriet, and F. Albarede, The evolution of Mauna Kea volcano, Hawaii: Petrogenesis of tholeiitic and alkalic basalts, *J. Geophys. Res.*, *96*, 14,347-14,375, 1991.

Frey, F. A., M. O. Garcia, and M. F. Roden, Geochemical characteristics of Koolau volcano: Implications of intershield geochemical differences among Hawaiian volcanoes, *Geochim. Cosmochim. Acta*, *58*, 1441-1462, 1994.

Garcia, M. O., Petrography, olivine, and glass chemistry of lavas from the Hawaii Scientific Drilling Project, *J. Geophys. Res.*, this issue.

Garcia, M. O., D. Muenow, and K. E. Aggley, Major element, volatile, and stable isotopic geochemistry of Hawaiian submarine tholeiitic glasses, *J. Geophys. Res.*, *94*, 10,525-10,538, 1989.

Garcia, M. O., J. M. Rhodes, E. W. Wolfe, G. E. Ulrich, and R. A. Ho, Petrology of lavas from episodes 2-47 of the Puu Oo eruption of Kilauea volcano, Hawaii: Evaluation of magmatic processes, *Bull. Volcanol.*, *55*, 1-16, 1992.

Garcia, M. O., T. P. Hulsebosch, and J. M. Rhodes, Olivine-rich submarine basalts from the southwest rift zone of Mauna Loa volcano: Implications for magmatic processes and geochemical evolution, in *Mauna Loa Revealed: Structure, Composition, History, and Hazards, Geophys. Monogr. Ser.*, vol. 92, edited by J.M. Rhodes and J.P. Lockwood, pp. 219-239, AGU, Washington D.C., 1995.

Geist, D. J., An appraisal of melting processes and the Galapagos hotspot: Major and trace element evidence, *J. Volcanol. Geotherm. Res.*, *52*, 65-82, 1992.

Hart, S. R., and K. E. Davis, Nickel partitioning between olivine and silicate melt, *Earth Planet. Sci. Lett.*, *40*, 203-219, 1978.

Hawaii Scientific Drilling Project, Core-Logs, edited by E. Stolper, and M. Baker, 471 pp., Calif. Inst. of Tech., Pasadena, 1994.

Hirose, K., and I. Kushiro, Partial melting of dry peridotites at high pressures: Determination of compositions of melts segregated from peridotite using aggregates of diamond, *Earth Planet. Sci. Lett.*, *114*, 477-489, 1993.

Hofmann, A. W., Nb in Hawaiian magmas: Constraints on source composition and evolution, *Chem. Geol.*, *57*, 17-30, 1986.

Hofmann, A. W., and K. P. Jochum, Source characteristics derived from very incompatible trace elements in Mauna Loa and Mauna Kea basalts, Hawaii Scientific Drilling Project, *J. Geophys. Res.*, this issue.

Hofmann, A. W., M. D. Feigenson, and I. Raczek, Case studies on the origin of basalt, III, Petrogenesis of the Mauna Ulu eruption, Kilauea, 1969-1971, *Contrib. Mineral. Petrol.*, *88*, 24-35, 1984.

Hofmann, A. W., M. D. Feigenson, and I. Raczek, Kohala revisited, *Contrib. Mineral. Petrol.*, *95*, 114-122, 1987.

Kennedy, A. K., S.-T. Kwon, F. A. Frey, and H. B. West, The isotopic composition of postshield lavas from Mauna Kea volcano, Hawaii, *Earth Planet. Sci. Lett.*, *103*, 339-353, 1991.

Kinzler, R. J., and T. L. Grove, Primary magmas of mid-ocean ridge basalts, 2, Applications, *J. Geophys. Res.*, *97*, 6907-6926, 1992.

Kinzler, R. J., T. L. Grove, and S. I. Recca, An experimental study on the effect of temperature and melt composition on the partitioning of nickel between olivine and silicate melt, *Geochim. Cosmochim. Acta*, *54*, 1255-1265, 1990.

Kurz, M. D., and D. P. Kammer, Isotopic evolution of Mauna Loa volcano, *Earth Planet. Sci. Lett.*, *103*, 257-269, 1991.

Kurz, M. D., M. O. Garcia, F. A. Frey, and P. A. O'Brien, Temporal helium isotopic variations within Hawaiian volcanoes: Basalts from Mauna Loa and Haleakala, *Geochim. Cosmochim. Acta*, *51*, 2905-2914, 1987.

Kurz, M. D., T. C. Kenna, D. P. Kammer, J. M. Rhodes, and M. O. Garcia, Isotopic evolution of Mauna Loa volcano: A view from the submarine southwest rift, in *Mauna Loa Revealed: Structure, Composition, History, and Hazards, Geophys. Monogr. Ser.*, vol. 92, edited by J. M. Rhodes and J. P. Lockwood, pp. 289-306, AGU, Washington, D. C., 1995.

Kurz, M. D., T. C. Kenna, J. C. Lassiter, and D. J. DePaolo, Helium isotopic evolution of Mauna Kea volcano: First results from the 1-km drill core, *J. Geophys. Res.*, this issue.

Langenheim, V. A. M., and D. A. Clague, The Hawaiian-Emperor Volcanic Chain, II, Stratigraphic framework of volcanic rocks of the Hawaiian Islands, *U.S. Geol. Surv. Prof. Pap.*, *1350*, 55-84, 1987.

Langmuir, C. H., E. M. Klein, and T. Plank, Petrological systematics of mid-ocean ridge basalts: Constraints on melt generation beneath ocean ridges, in *Mantle Flow and Melt Generation at Mid-Ocean Ridges, Geophys. Monogr. Ser.* vol. 71, edited by J. P. Morgan, D. K. Blackman, and J. M. Sinton, AGU, pp. 183-280, Washington, D.C., 1992.

Lanphere, M. A., and F. A. Frey, Geochemical evolution of Kohala volcano, Hawaii, *Contrib. Mineral. Petrol.*, *95*, 100-113, 1987.

Lassiter, J. C., D. J. DePaolo, and M. Tatsumoto, Isotopic evolution of Mauna Kea volcano: Results from the initial phase of the Hawaii Scientific Drilling Project, *J. Geophys. Res.*, this issue, 1995.

Le Bas, M. J., R. W. Le Maitre, and A. R. Woolley, The construction of the total alkali-silica chemical classification of volcanic rocks, *Mineral. Petrol.*, *46*, 1022, 1992.

Lipman, P. W., J. M. Rhodes, and G. B. Dalrymple, The Ninole basalt-Implications for the structural evolution of Mauna Loa volcano, Hawaii, *Bull. Volcanol.*, *53*, 1-19, 1990.

Macdonald, G. A., and T. Katsura, Chemical composition of Hawaiian lavas, *J. Petrol.*, *5*, 82-133, 1964.

Macdonald, G. A., A. T. Abbott, and F. L. Peterson, *Volcanoes in the Sea: The Geology of Hawaii*, Univ. of Hawaii Press, Honolulu, 1983.

Moore, J. G., and D. L. Peck, Submarine lavas from the east rift zone of Mauna Kea, Hawaii (abstract), *Spec. Pap. Geol. Soc. Am.*, *87*, 218, 1966.

Morse, S. A., J. M. Rhodes, and K. M. Nolan, Redox effect on the partitioning of nickel in olivine, *Geochim. Cosmochim. Acta*, *55*, 2373-2378, 1991.

Pietruszka, A. J., and M. Garcia, The historical summit lavas of Kilauea volcano (1790-1982 A.D.): Geochemical variations in space and time, *Eos Trans. AGU*, *75* (44), Fall Meet. Suppl., 712, 1994.

Plank, T., and C. H. Langmuir, Effects of the melting regime on the composition of the ocean crust, *J. Geophys. Res.*, *97*, 19,749-19,770, 1992.

Rhodes, J. M., Geochemistry of the 1984 Mauna Loa eruption: Implication for magma storage and supply, *J. Geophys. Res.*, *93*, 4453-4466, 1988.

Rhodes, J. M., Geochemical stratigraphy of lava flows sampled by the Hawaii Scientific Drilling Project, *J. Geophys. Res.*, this issue.

Rhodes, J. M., and S. R. Hart, Episodic trace element and isotopic variations in historical Mauna Loa lavas: Implications for magma and plume dynamics, in *Mauna Loa Revealed: Structure, Composition, History, and Hazards, Geophys. Monogr. Ser.*, vol. *92*, edited by J. M. Rhodes and J. P. Lockwood, pp. 263-288, AGU, Washington, D.C., 1995.

Rhodes, J. M., K. P. Wenz, C. A. Neal, J. W. Sparks, and J. P. Lockwood, Geochemical evidence for invasion of Kilauea's plumbing system by Mauna Loa magma, *Nature*, *337*, 257-260, 1989.

Ribe, N. M., Dynamical geochemistry of the Hawaiian plume, *Earth Planet. Sci. Lett.*, *88*, 37-46, 1988.

Ribe, N. M., and M. O. Smooke, A stagnation point flow model for melt extraction from a mantle plume, *J. Geophys. Res.*, *92*, 6437-6443, 1987.

Roden, M. F., T. Trull, S. R. Hart, and F. A. Frey, New He, Sr, Nd and Pb isotopic constraints on the constitution of the Hawaiian plume: Results from Koolau volcano, Oahu, Hawaii, *Geochim. Cosmochim. Acta, 58*, 1431-1440, 1994,

Scarrow, J. H., and K. G. Cox, Basalts generated by decompressive adiabatic melting of a mantle plume: A case study from the Isle of Skye, NW Scotland, *J. Petrol.*, *36*, 3-22, 1995.

Sharp, W. D., B. D. Turrin, P. R. Renne, and M. A. Lanphere, The $^{40}Ar/^{39}Ar$ and K/Ar dating of lavas from the Hilo 1-km core hole, Hawaii Scientific Drilling Project, *J. Geophys. Res.*, this issue.

Spengler, S. R., and M. O. Garcia, Geochemistry of the Hawi lavas, Kohala volcano, Hawaii, *Contrib. Mineral. Petrol.*, *99*, 90-104, 1988.

Sun, S.-S., and W. F. McDonough, Chemical and isotopic systematics of oceanic basalts: Implications for mantle composition and processes, in *Magmatism in the Ocean Basins*, edited by A. D. Saunders, and M. J. Norry, *Geol. Soc. Spec. Pub. London*, *42*, 313-345, 1989.

Takahashi, E., T. Shimazaki, Y. Tsuzaki, H. Yoshida, and K. Uto, Melting study of a peridotite KLB-1 to 6.5 GPa and Origin of basaltic magmas, *Philos. Trans. R. Soc. London A*, *342*, 105-120, 1993.

Tilling, R. I., T. L. Wright, and H. T. Millard, Trace-element chemistry of Kilauea and Mauna Loa lava in space and time: A reconnaissance, *U.S. Geol. Surv. Prop. Pap.*, *1350*, 641-689, 1987.

Wagner, T. P., and T. L. Grove, Primary magmas of the Hawaiian plume: Experimental evidence bearing on the plume paradox, *Eos Trans. AGU, 73, Fall Meet. Suppl.*, 615, 1992.

Walter, M. J., and D. C. Presnall, Melting behavior of simplified lherzolite in the system $CaO-MgO-Al_2O_3-SiO_2-Na_2O$ from 7 to 35 kbar, *J. Petrol.*, *35*, 329-360, 1994.

Watson, S., Rare earth element inversions and percolation models for Hawaii, *J. Petrol.*, *34*, 763-783, 1993.

Watson, S., and D. McKenzie, Melt generation by plumes: A study of Hawaiian volcanism, *J. Petrol.*, *32*, 501-537, 1991.

West, H. B., and W. P. Leeman, Isotopic evolution of lavas from Haleakala crater, Hawaii, *Earth Planet. Sci. Lett.*, *84*, 211-225, 1987.

West, H. B., and W. P. Leeman, The open-system geochemical evolution of alkalic cap lavas from Haleakala crater, Hawaii, U.S.A., *Geochim. Cosmochim. Acta, 58*, 773-796, 1994.

West, H. B., M. O. Garcia, F. A. Frey, and A. Kennedy, Nature and cause of compositional variation among the alkalic cap lavas of Mauna Kea volcano, Hawaii, *Contrib. Mineral. Petrol.*, *100*, 383-397, 1988.

Wolfe, E. W., W. S. Wise, and G. B. Dalrymple, Geology and petrology of Mauna Kea volcano, Hawaii: A study of postshield volcanism, *U.S. Geol. Surv. Prof. Pap.*, *1557*, in press, 1995.

Wright, T. L., Origin of Hawaiian tholeiite: A metasomatic model, *J. Geophys. Res.*, *89*, 3233-3252, 1984.

Yang, H.-J., F. A. Frey, M. O. Garcia, and D. A. Clague, Submarine lavas from Mauna Kea volcano, Hawaii: Implications for Hawaiian shield-stage processes, *J. Geophys. Res.*, *99*, 15,577-15,594, 1994.

Yang, H.-J., R. J. Kinzler, and T. L. Grove, Experiments and models of anhydrous olivine-plagioclase-augite saturated melts from 0.001~10 kbar, *Contrib. Mineral. Petrol.*, in press, 1996.

F. A. Frey and H.-J. Yang, Department of Earth, Atmospheric and Planetary Sciences, Massachusetts Institute of Technology, Cambridge, MA 02139-4307. (e-mail: fafrey@mit.edu)

M. O. Garcia, Department of Geology and Geophysics, SOEST, 2525 Correa Road, University of Hawaii at Manoa, Honolulu, HI 96822. (e-mail: garcia@soest.hawaii.edu)

J. M. Rhodes, Department of Geology and Geography, University of Massachusetts, Morrill Science Center, Box 35820, Amherst, MA 01003-5820. (e-mail: jmrhodes@eclogite.geo.umass.edu)